



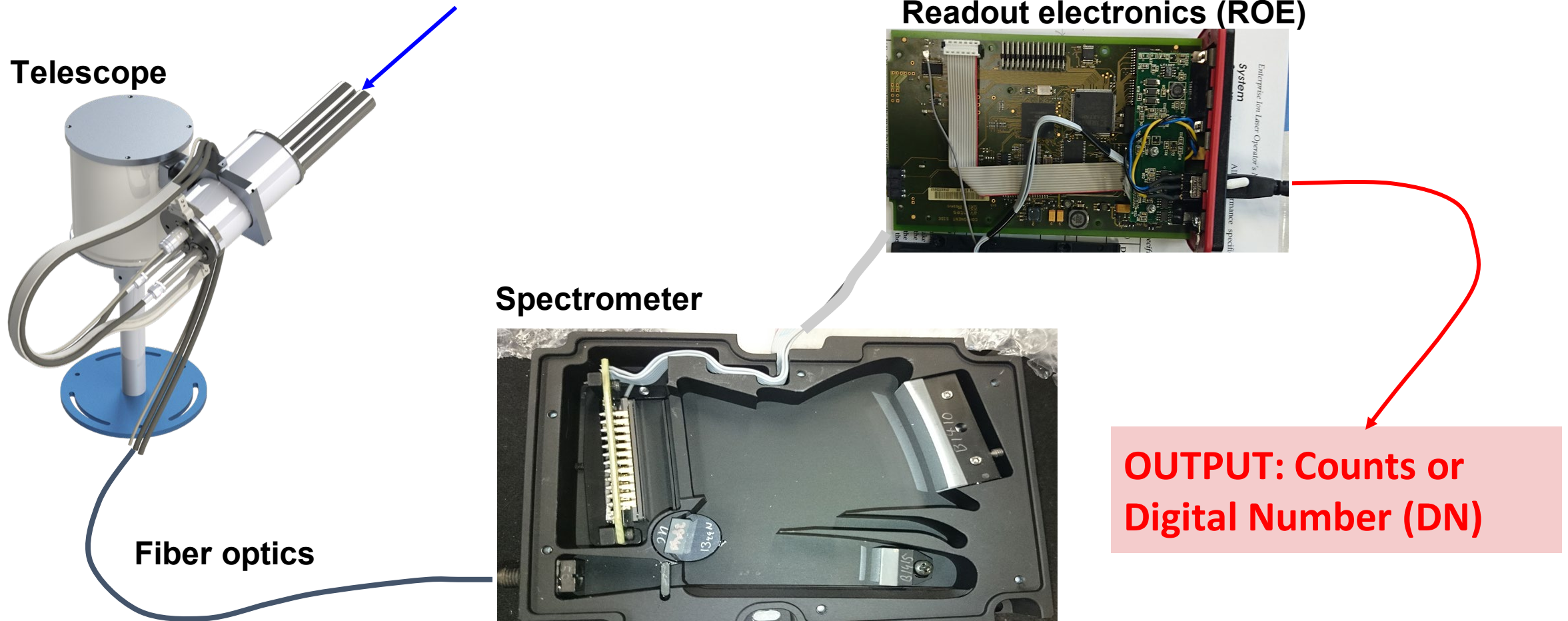
Instrument calibration part 1: Laboratory

Alexander Cede, LuftBlick

**Fifth Joint School on Atmospheric Composition
September 14 – 29, 2023**

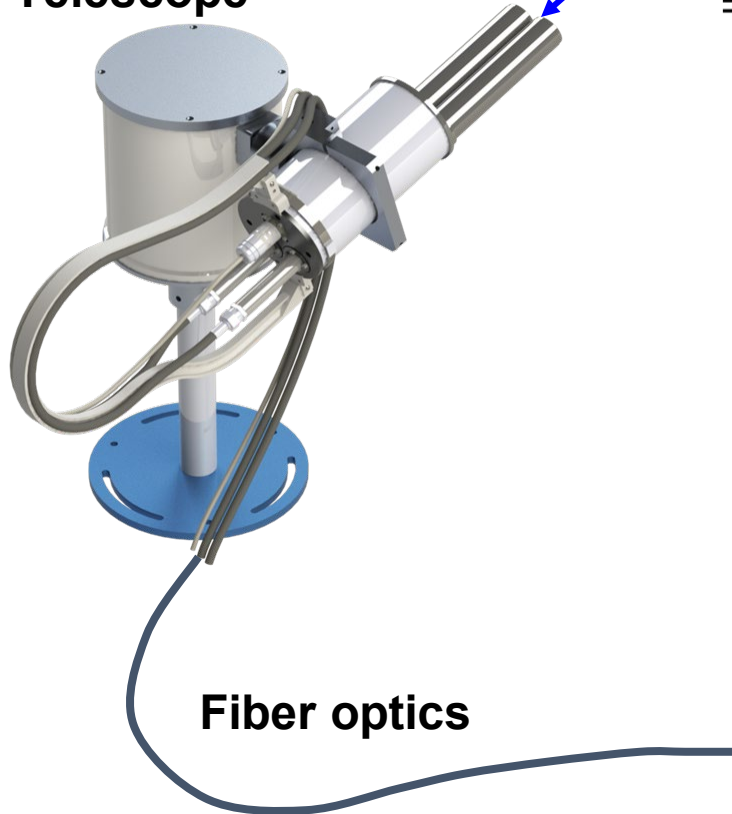
“Forward Direction”: From input flux to digital number

**INPUT: Spectral Irradiance [W/m²/nm] =
Energy received per time interval (J/s=W) per area (m²) per wavelength interval (nm)**

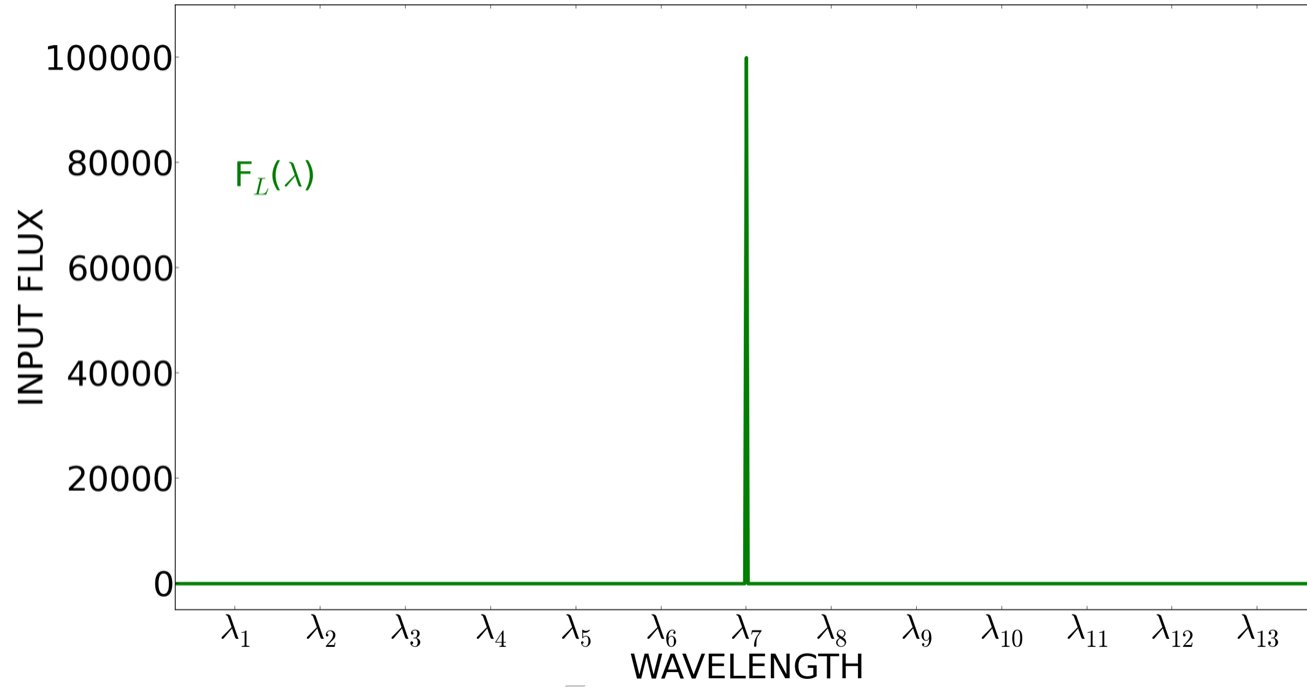


→ Follow a monochromatic input

Telescope



Fiber optics



Spectrometer



Flux at grating

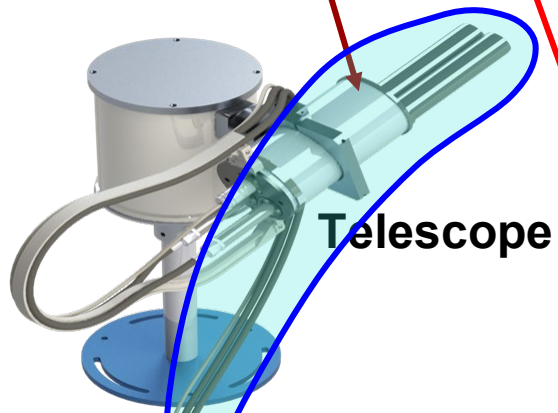


the telescope ...

the fiber ...

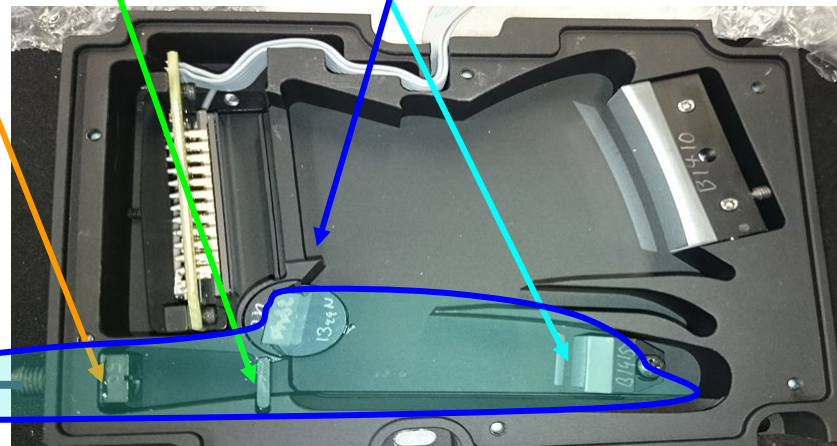
the entrance slit ...

an aperture ...

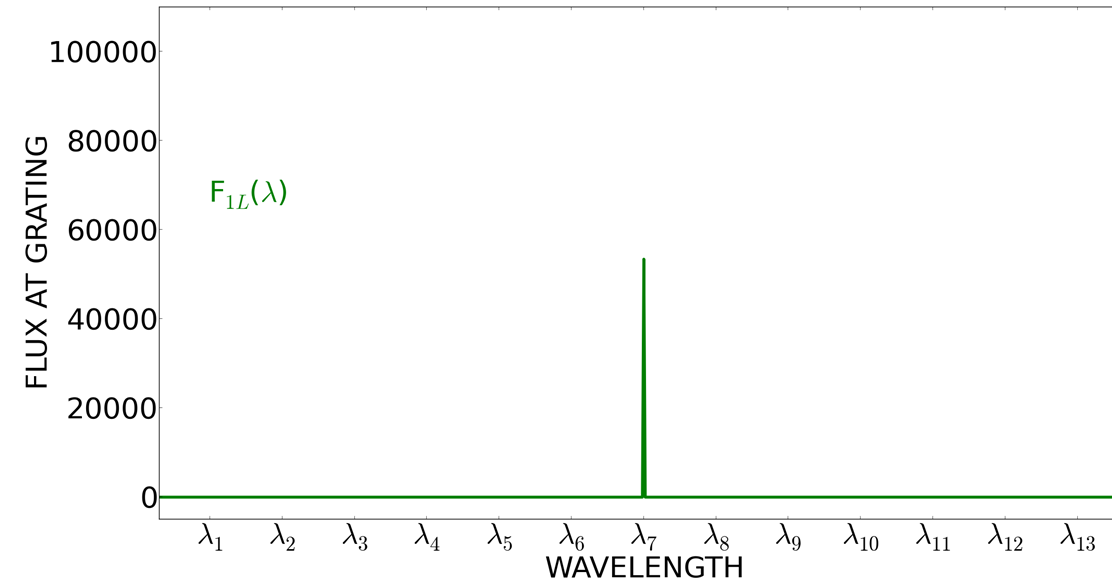


Telescope

Fiber optics



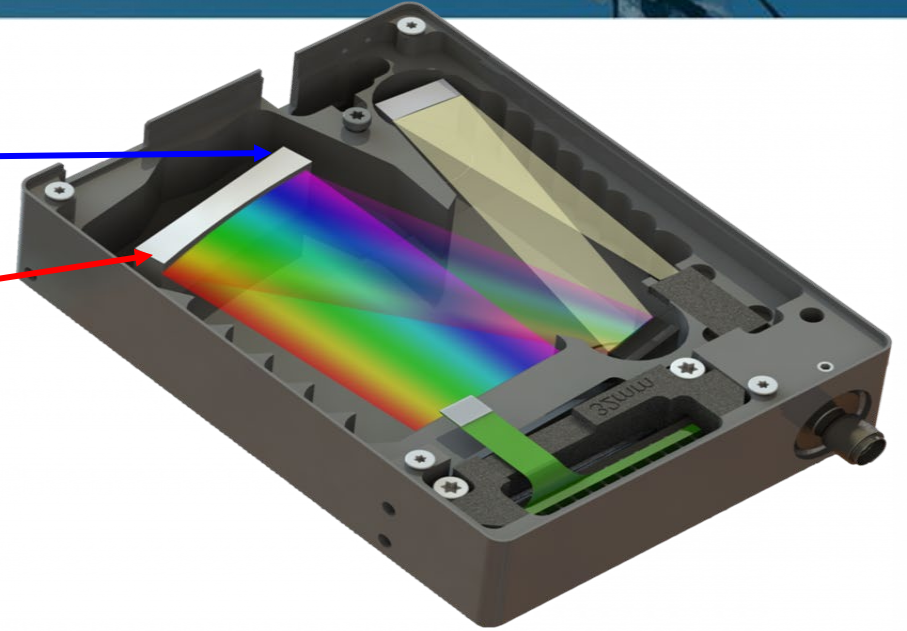
Spectrometer



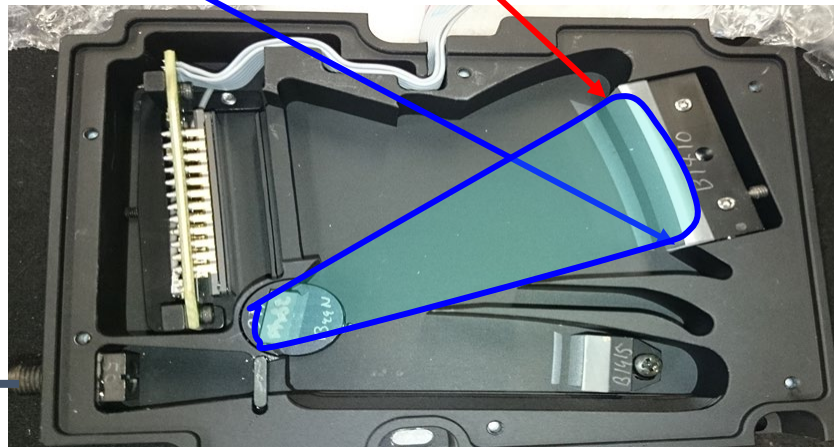
Dispersion

Lower wavelengths reach the 2nd mirror at one end.

Higher wavelengths reach the 2nd mirror at the other end.



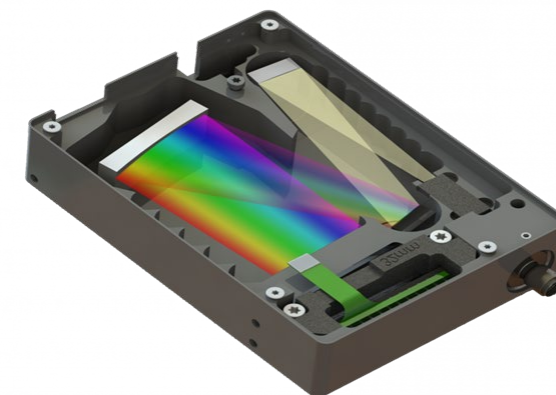
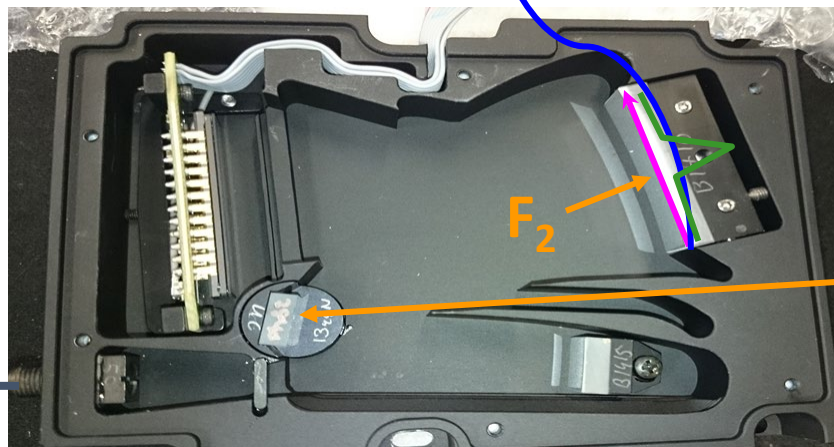
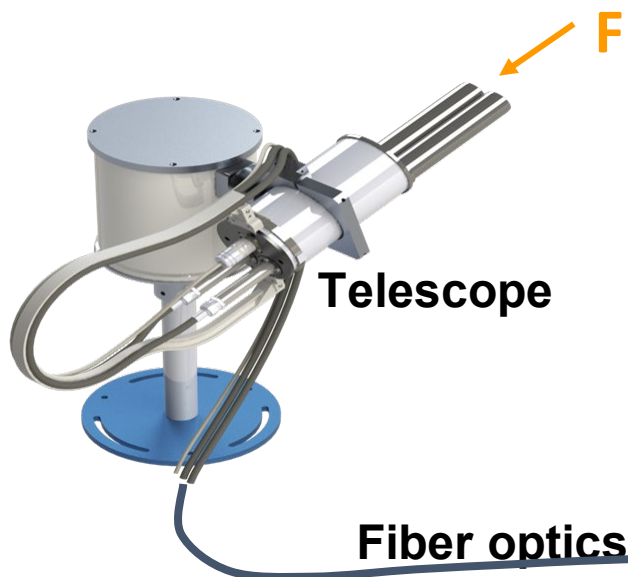
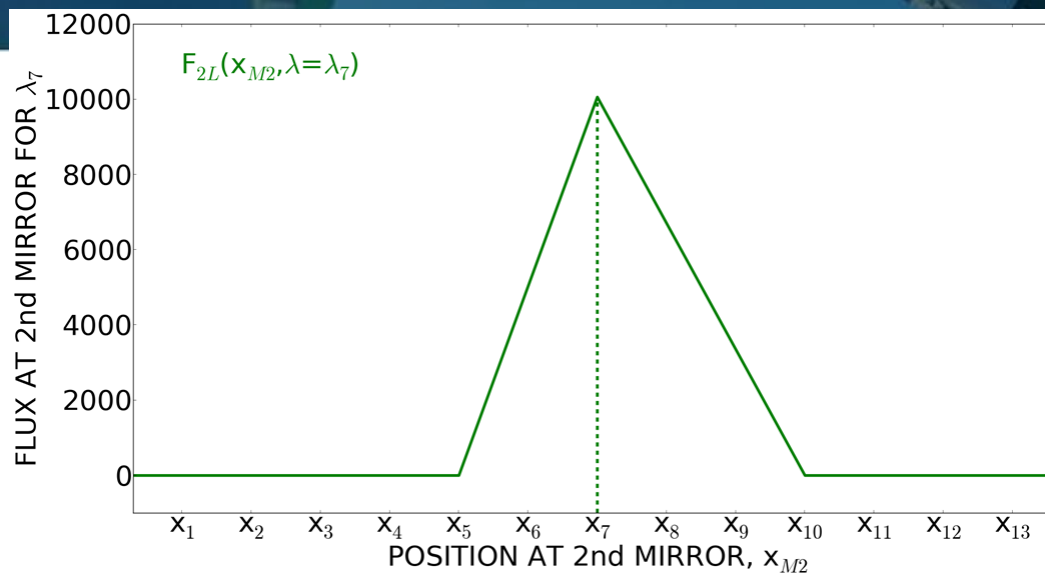
Fiber optics



Spectrometer

Flux at 2nd mirror

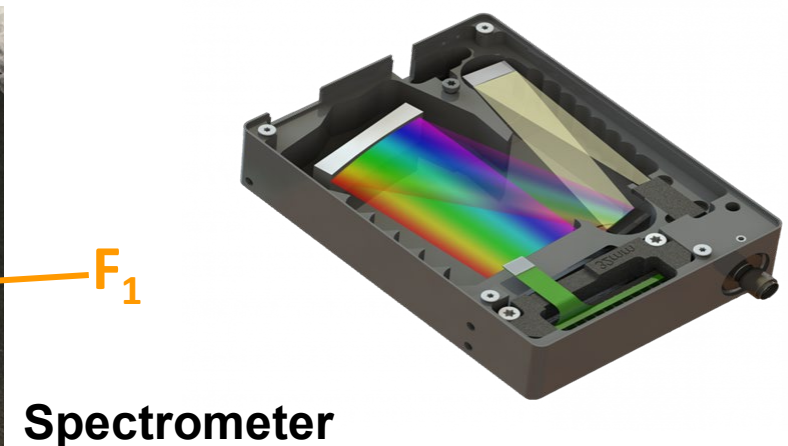
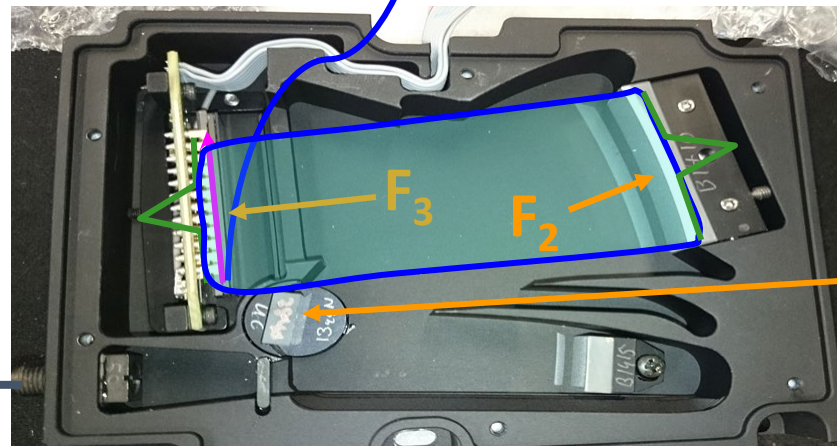
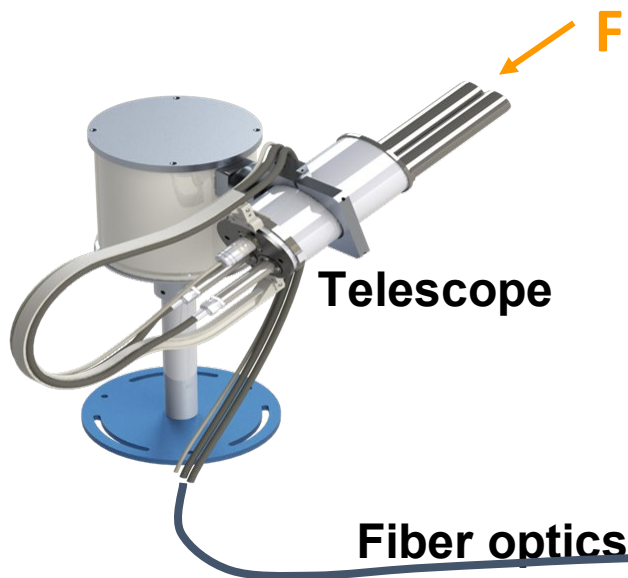
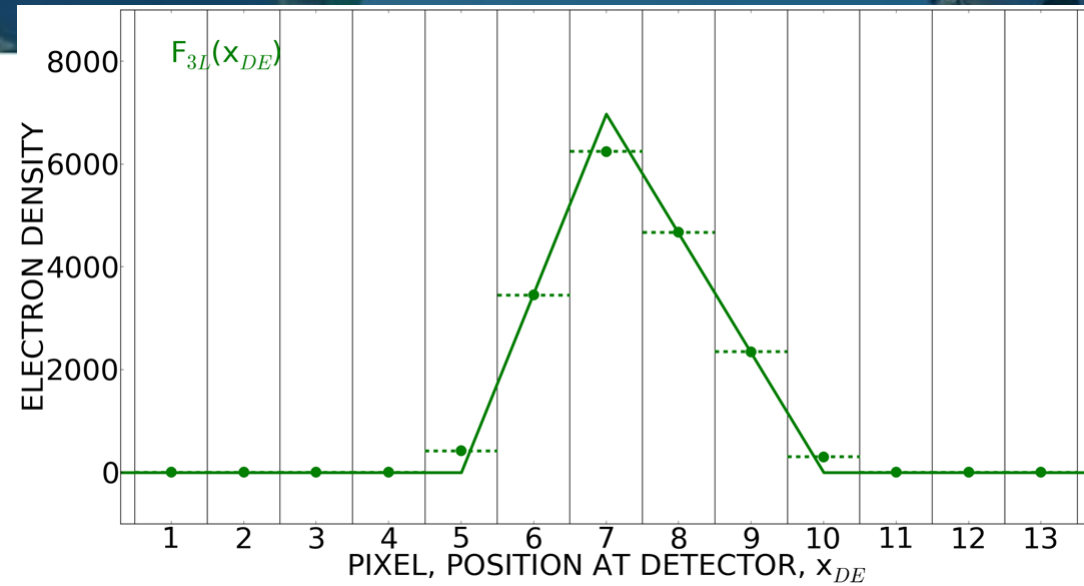
Monochromatic light distributes over
“some region” on the 2nd mirror.
Not a Delta-function anymore ...



Spectrometer

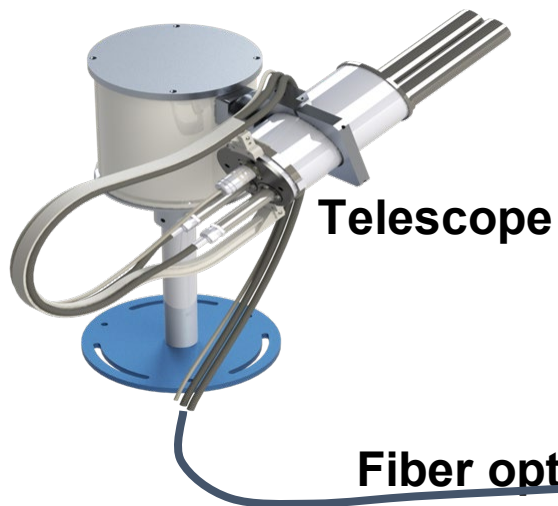
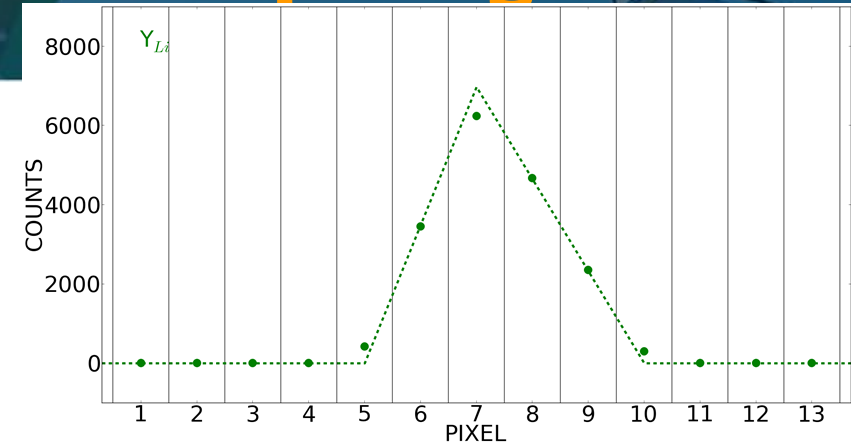
Flux at detector and electrons in detector

Flux at detector is binned into pixels

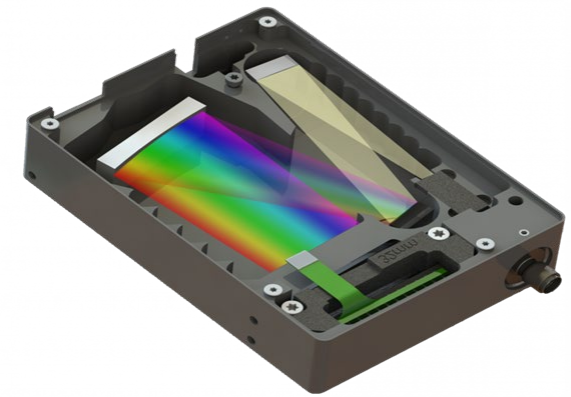


Transmission from detector to output signal

Counts for monochromatic input give "Slit (scatter) function".



Readout electronics



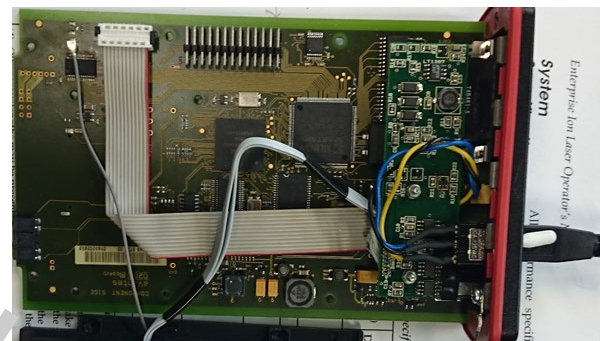
Spectrometer

“Backward Direction”: From digital number to flux



INPUT:
Spectral Irradiance

Calibration



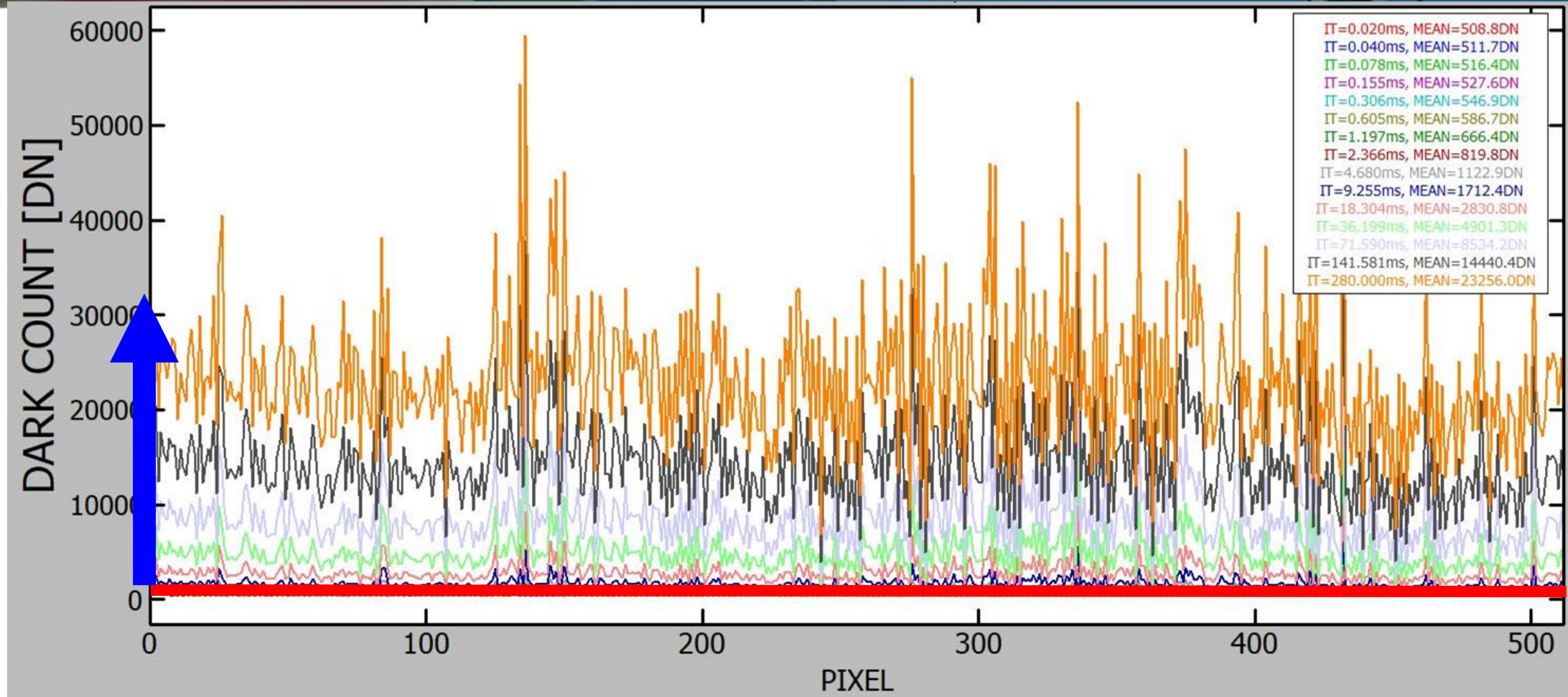
OUTPUT:
Counts

Effects of ROE (Readout electronics):
Dark offset, Dark slope, Gain, Linearity

Effects of detector:
Linearity, Latency, Quantum
efficiency, Flat field

Effects of Optics:
Transmissions (Grating efficiency, filters, mirrors,
...), Stray light, Temperature effects

Dark offset and slope



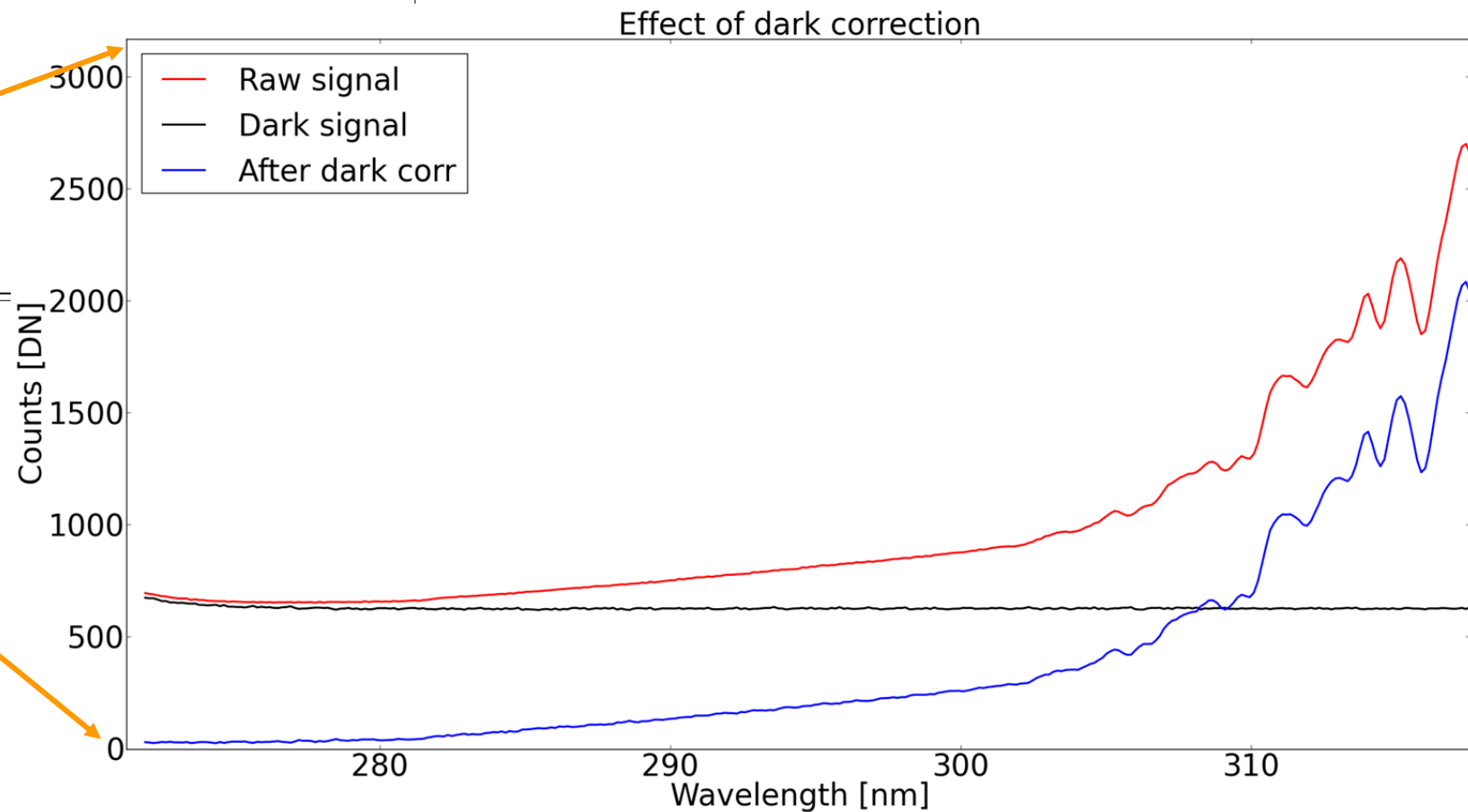
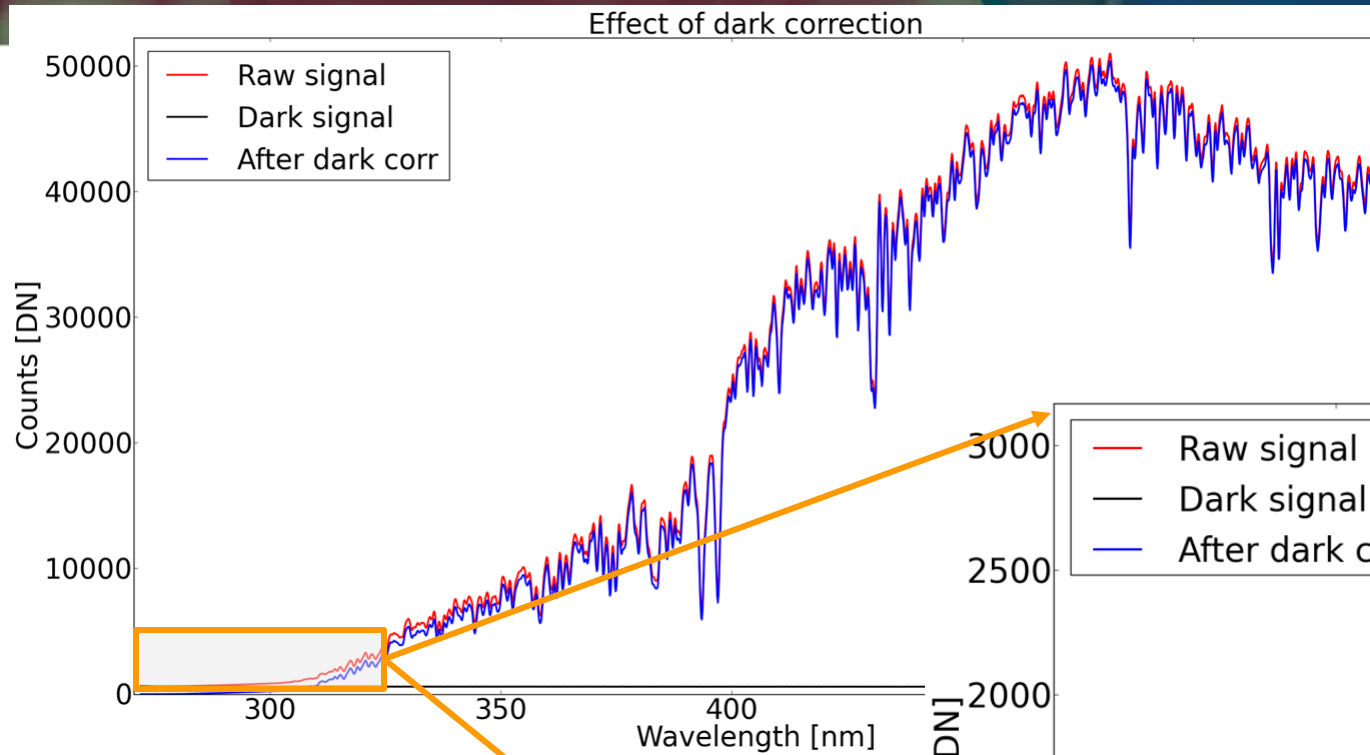
Dark Slope

(From thermal electrons)

Dark Offset

(From electronics)

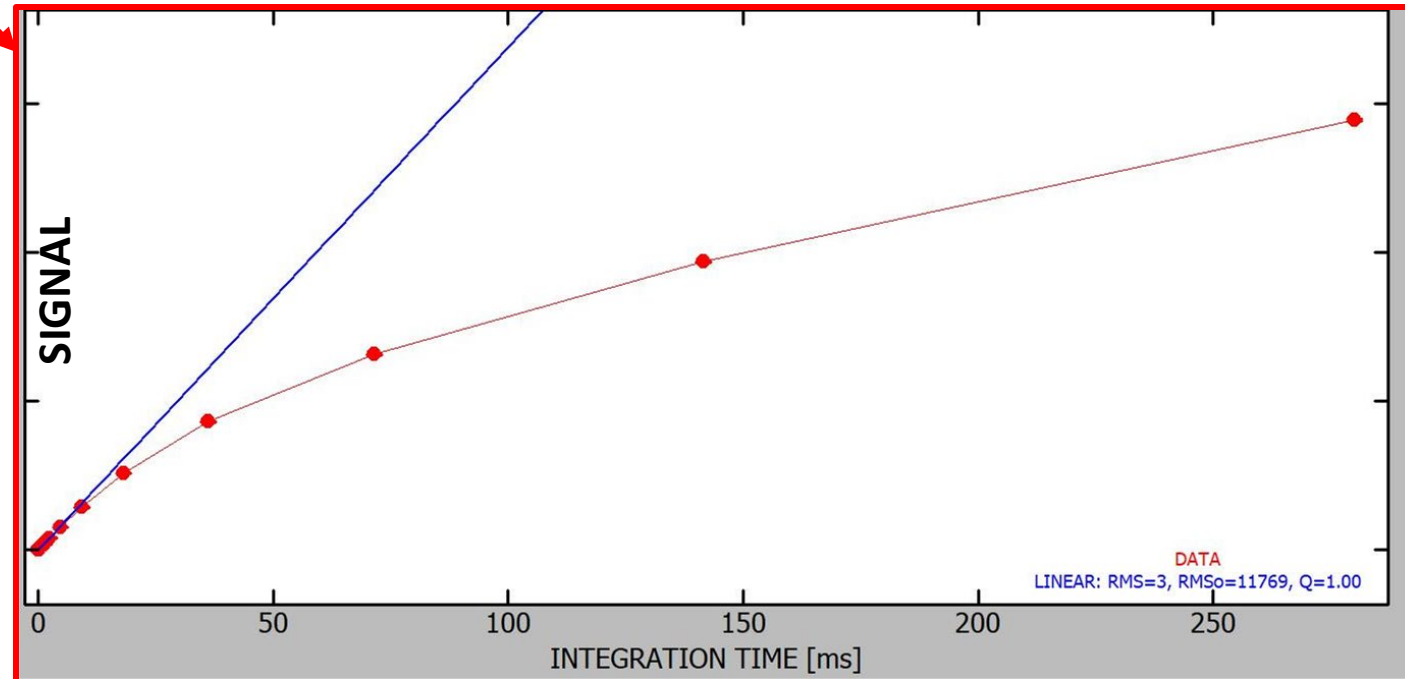
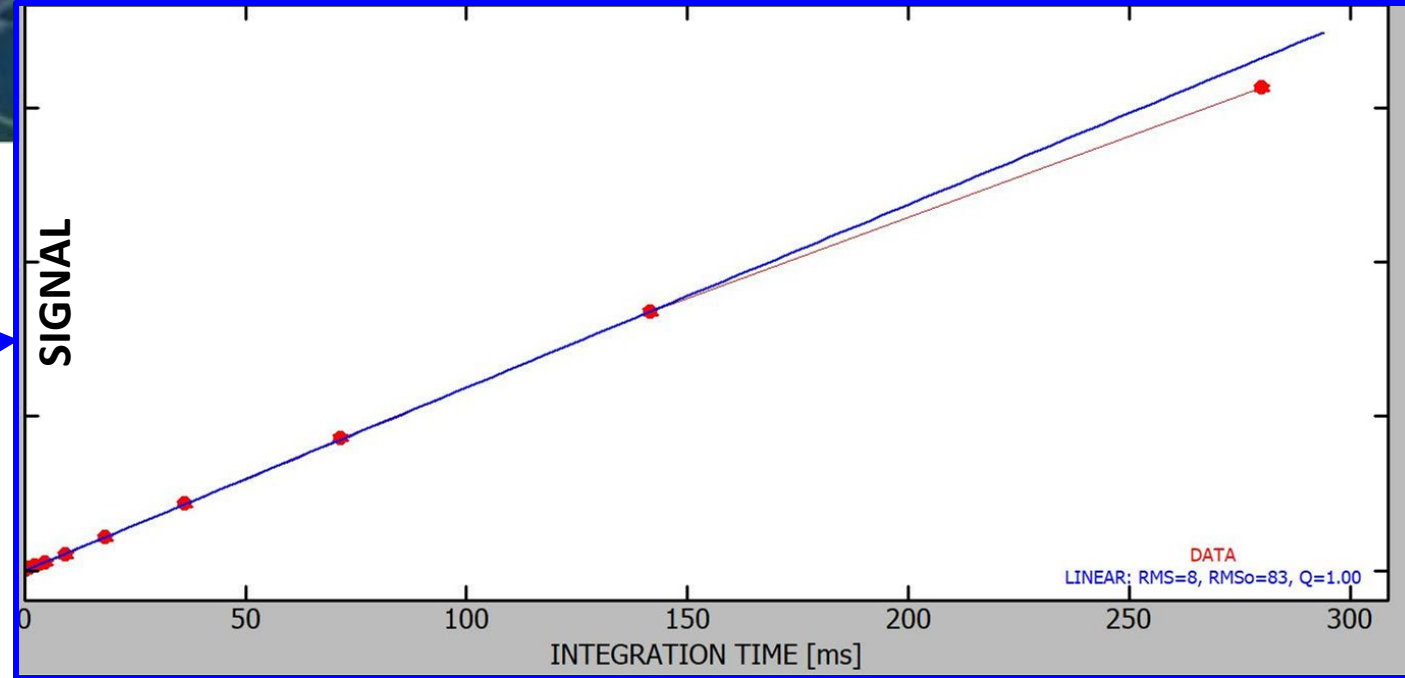
Dark correction



Linearity

(If you are lucky ...)
Dark & bright signals increase
~ linearly with light input

(If you are less lucky ...)
Your system is strongly non-linear



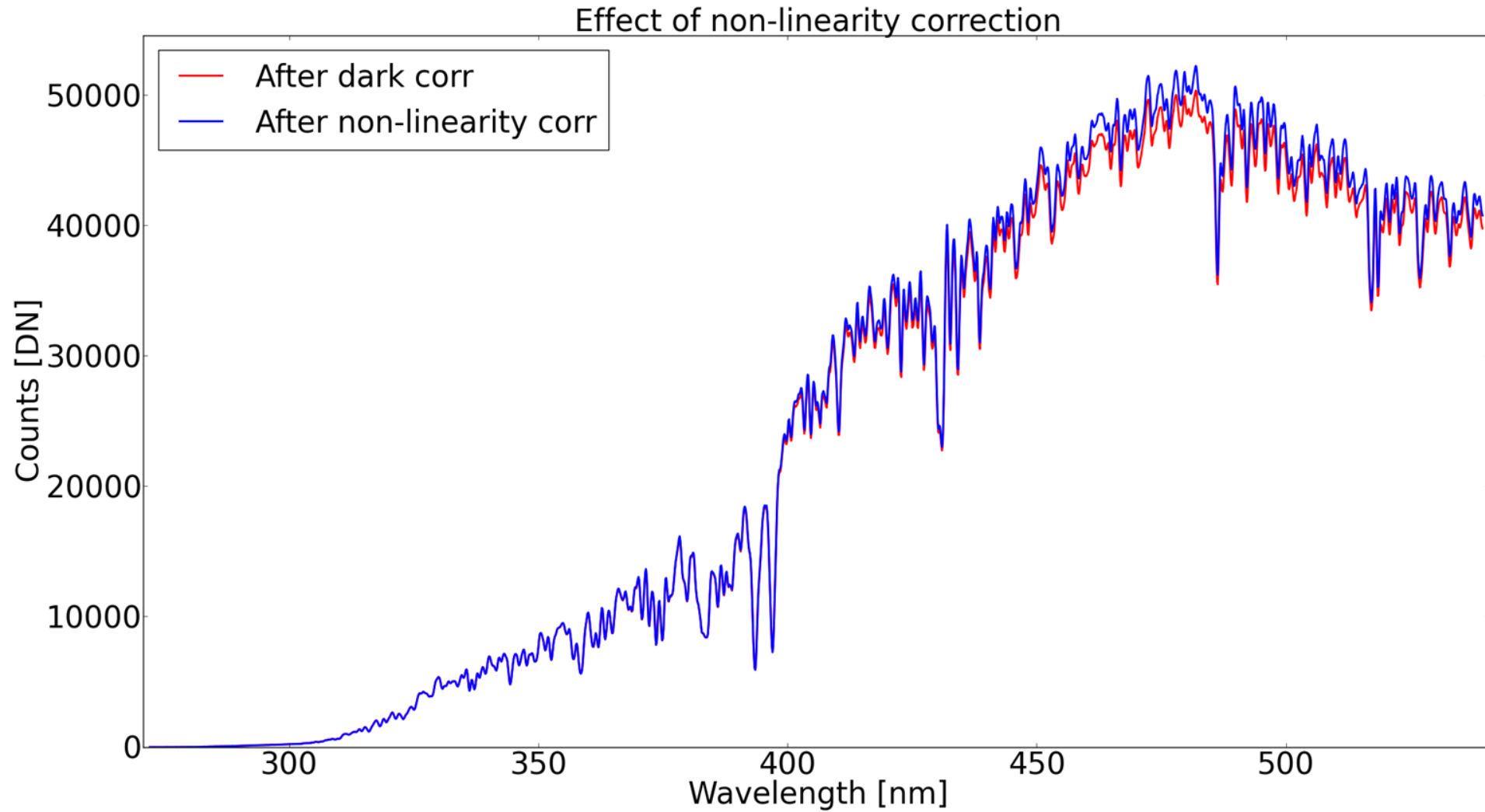
Non-linearity in Detector:

(Photon-induced or thermal) electron (e^-) accumulation differs from the e^- generation due to saturation and/or recombination.

Non-linearity in ROE:

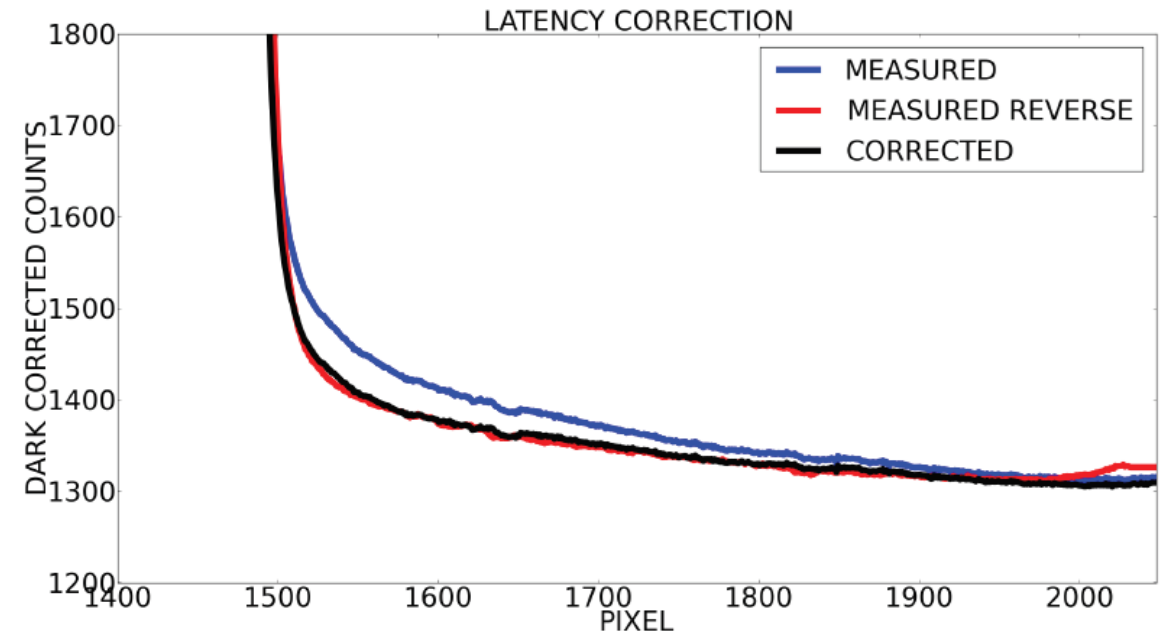
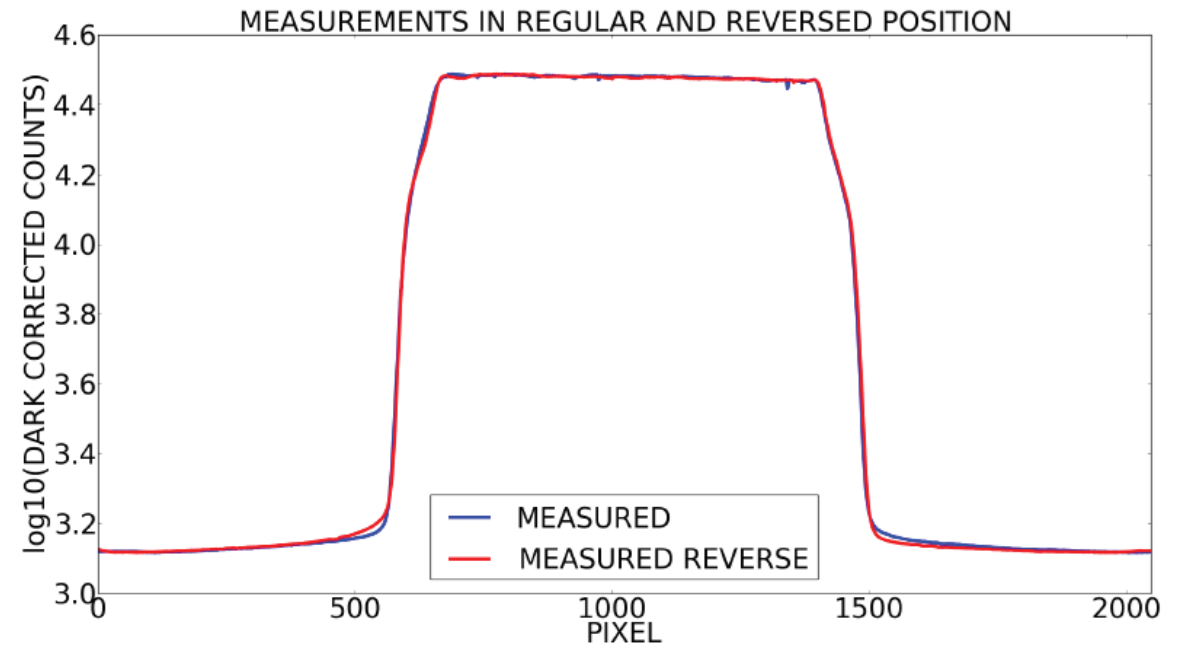
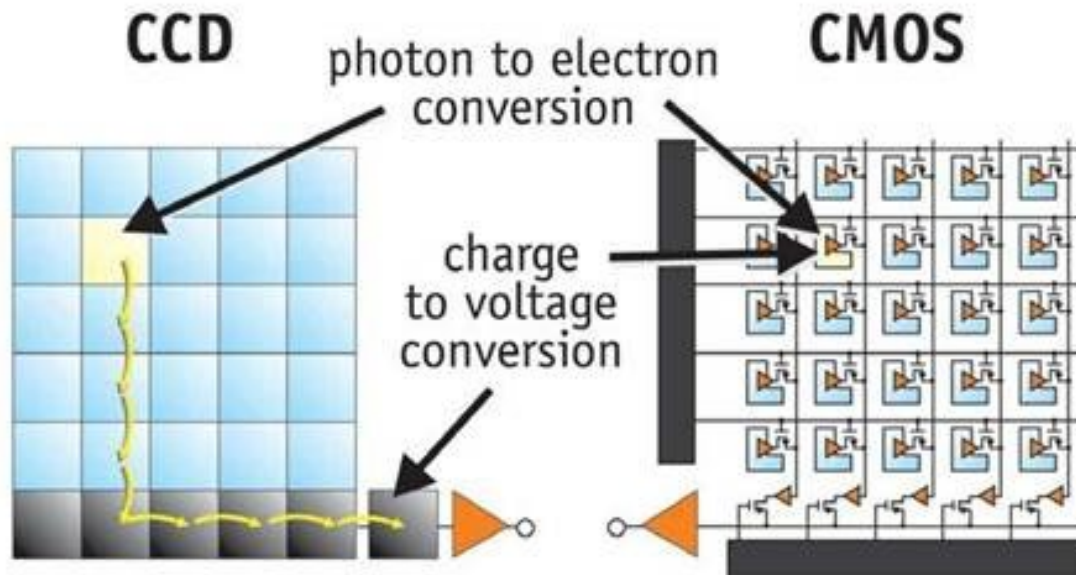
Caused by operational amplifier and AD-Converter

Linearity correction



Latency

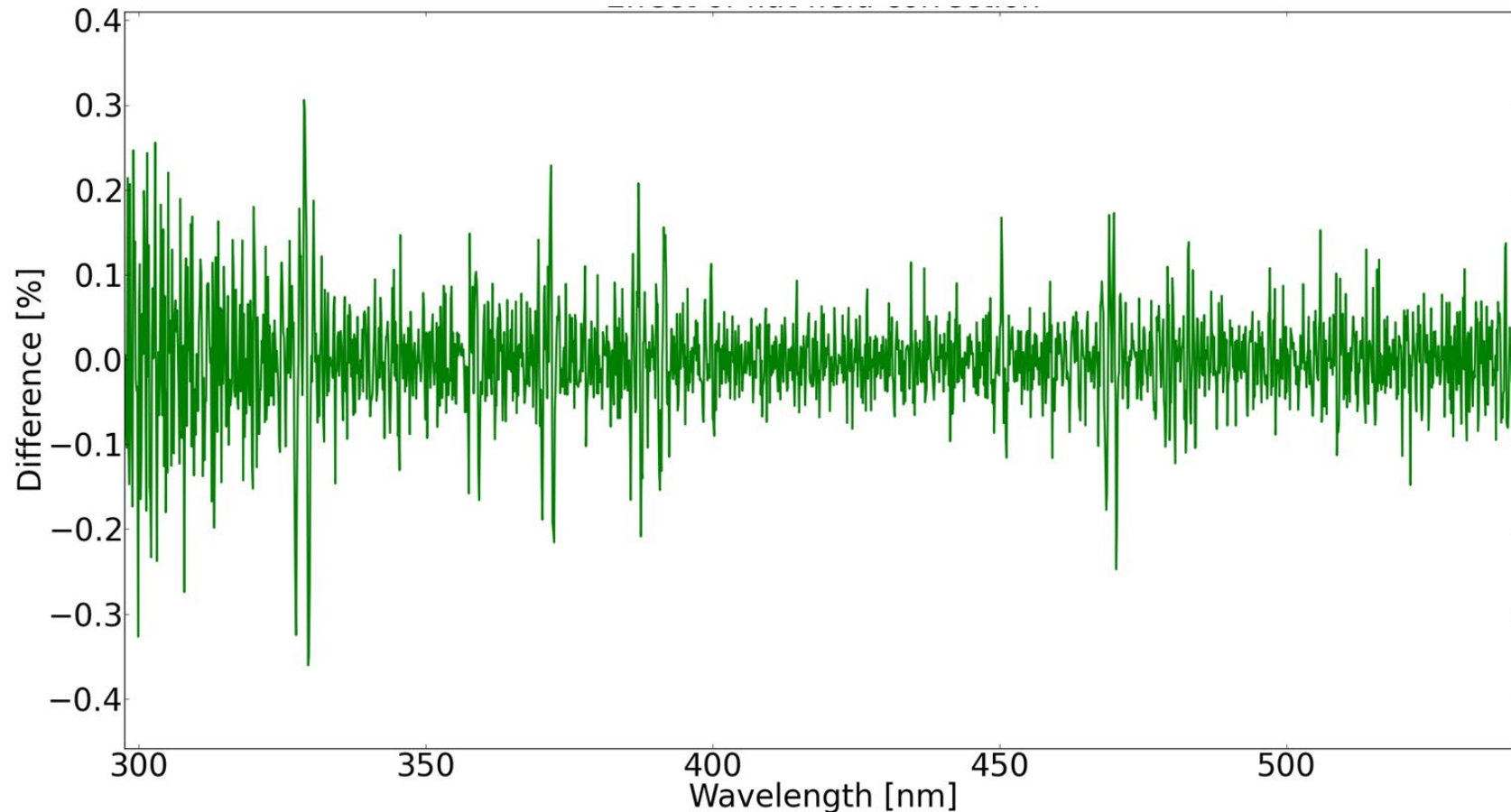
Readings in a pixel are influenced by the readings in the previously read pixel



Pixel Response Non Uniformity (PRNU)

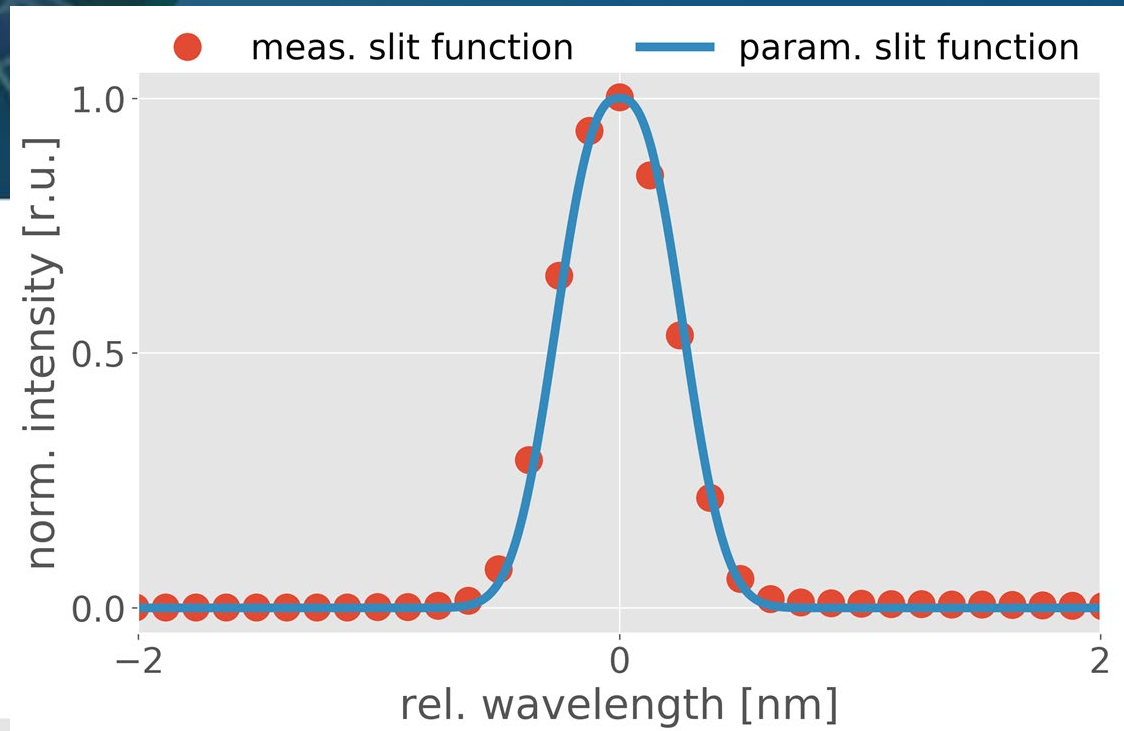
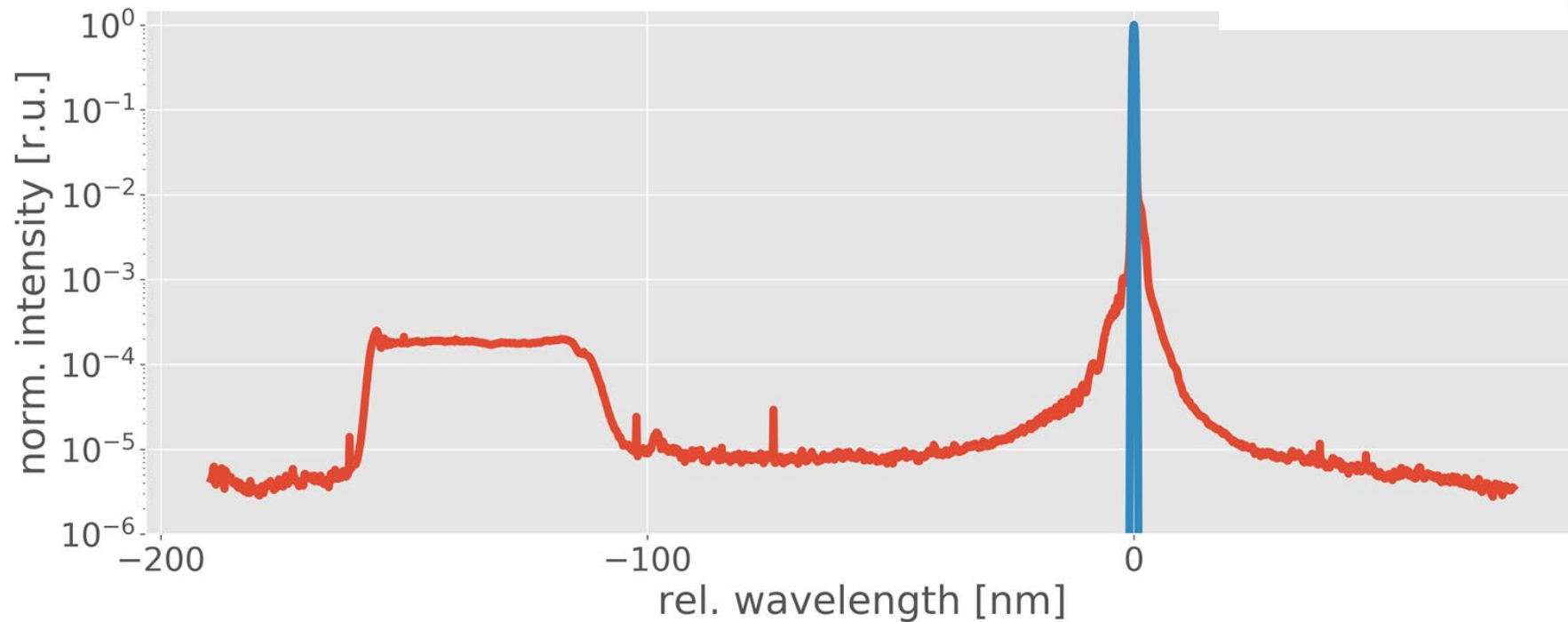
“What is the difference in the readings, if every pixel gets exactly the same input?”

For single pixels the PRNU is actually an effect of about $\pm 1\%$. Here it is reduced since for this CCD 64 single pixels are averaged in the reading.

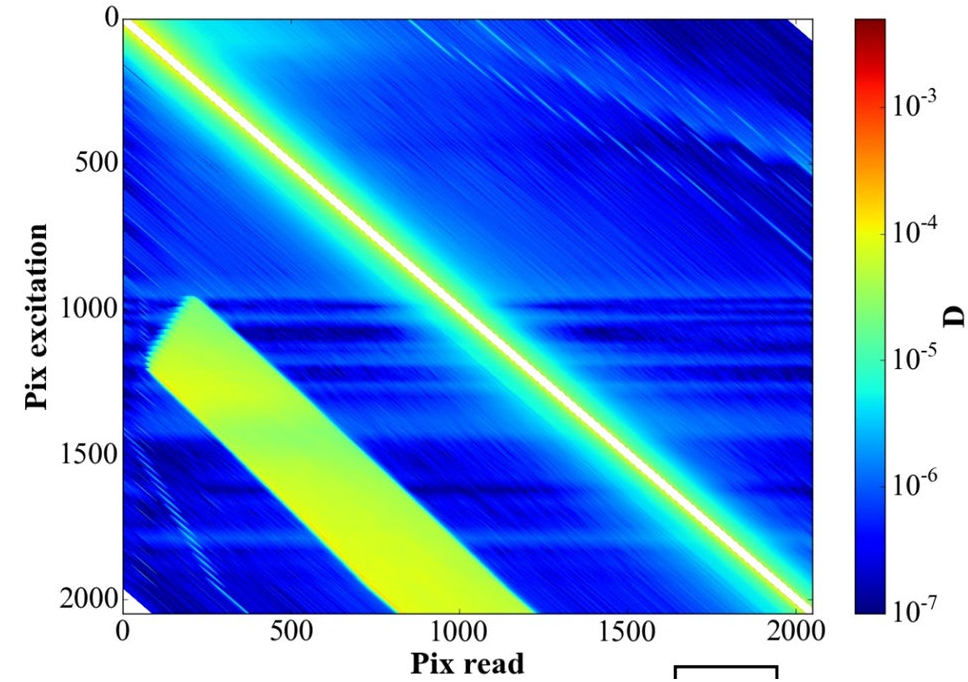
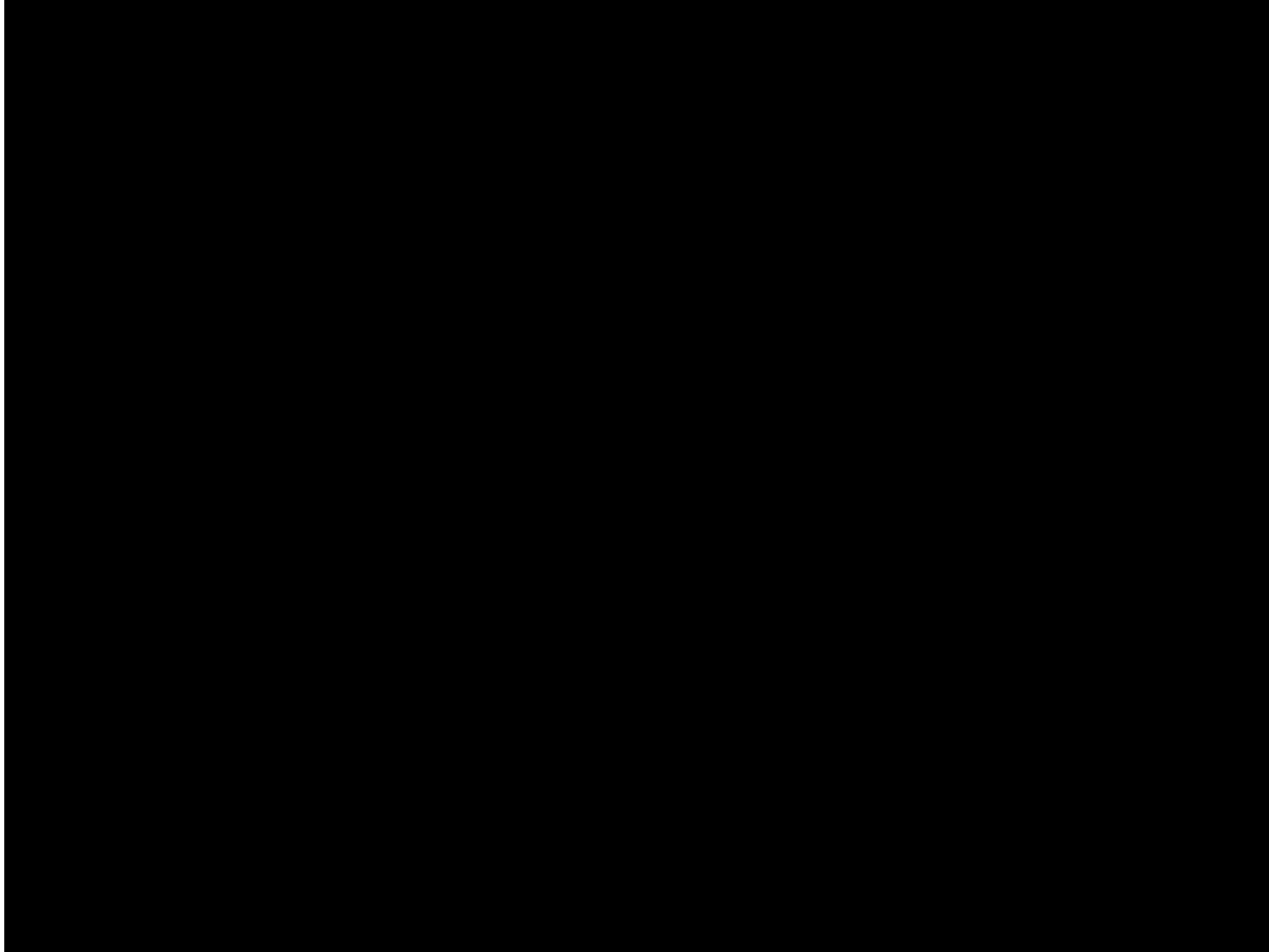


Spectral stray light

“Not all photons necessarily end up where they should.”



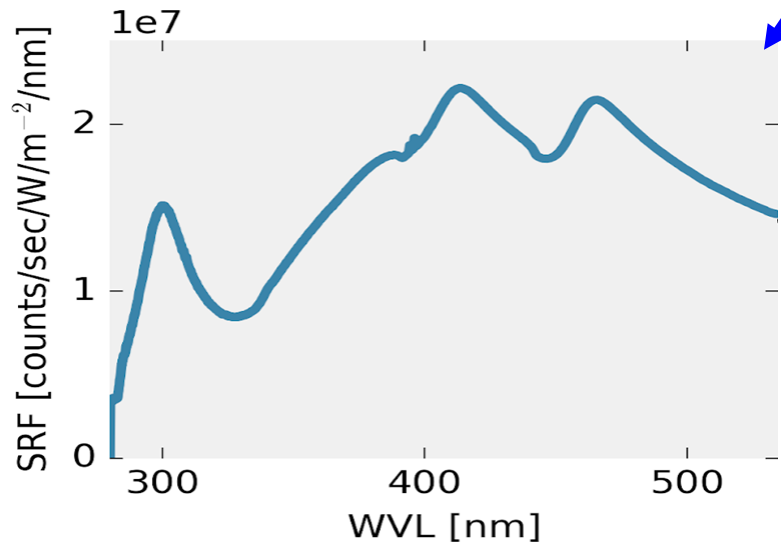
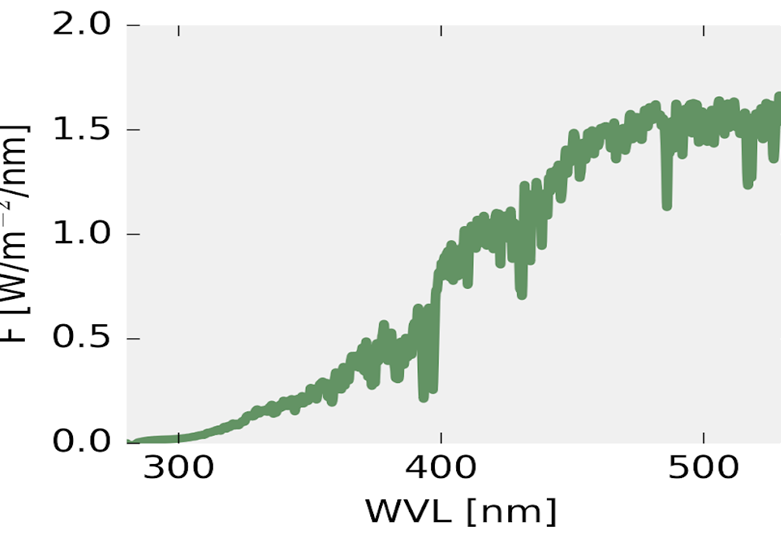
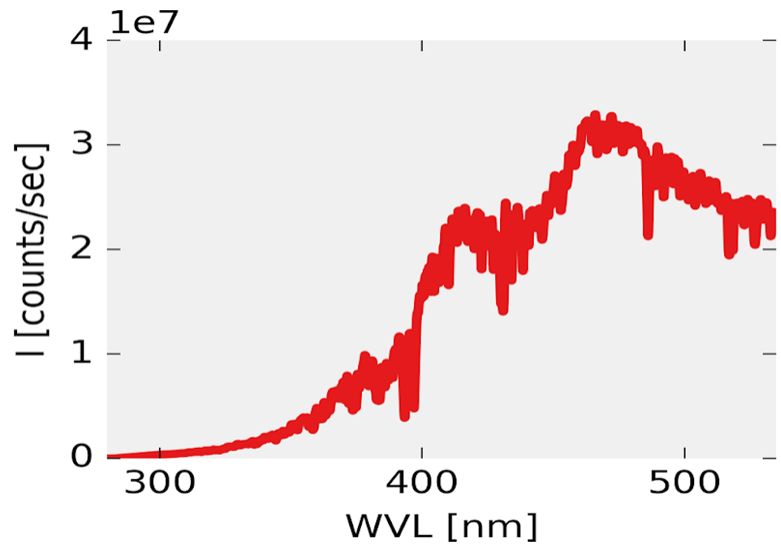
Full slit (scatter) function



Video compiled and thankfully provided by

- Julian Gröbner and
- Natalia Kouremeti

Spectral sensitivity

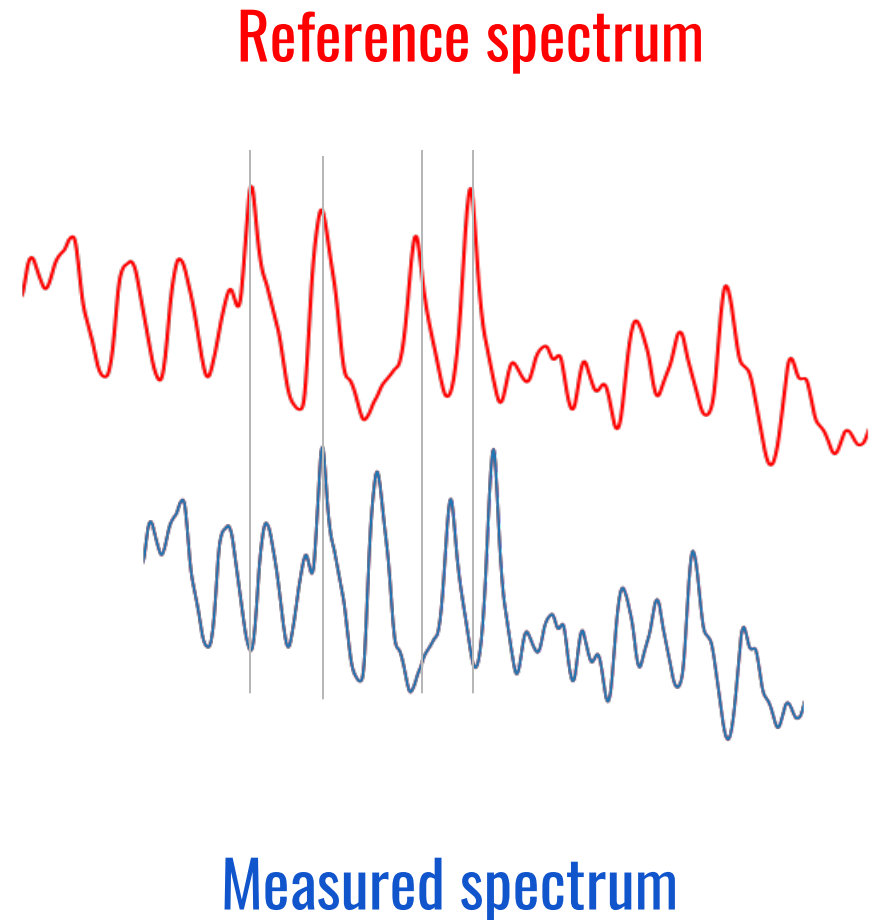


Combined effect
on transmission of
all optical
elements

- Windows
- Filters
- Fiber
- Mirrors
- Grating
- Detector
- ...

Dispersion and resolution changes

- In the lab we can determine the dispersion (which pixel corresponds to which wavelength) and resolution (width of slit function) of the system.
- However these **parameters usually change in the field** (temperature, instrument setup, ...).
- Due to the known structure of the solar spectrum, we can correct for this to some extent in the retrievals.
- More in Michel's talk about calibration techniques applied in the field ...



The background is a collage of scientific and atmospheric imagery. On the left, a white line-art satellite is shown against a colorful, abstract map of the Earth. On the right, a blue-toned image shows a vertical atmospheric instrument or probe. A large, semi-transparent globe is centered in the background, with a white lightning bolt striking across it. The overall color palette is dominated by blues, greens, and yellows, with some red and orange accents in the abstract map.

Instrument calibration part 2: In the field

Michel van Roozendael, BIRA-IASB

Fifth Joint School on Atmospheric Composition
September 14 – 29, 2023

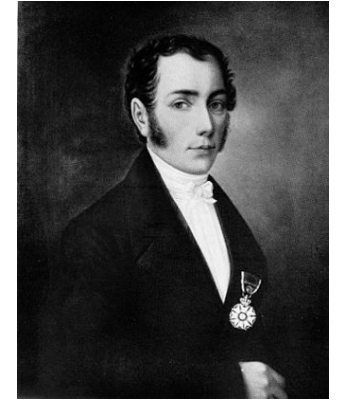
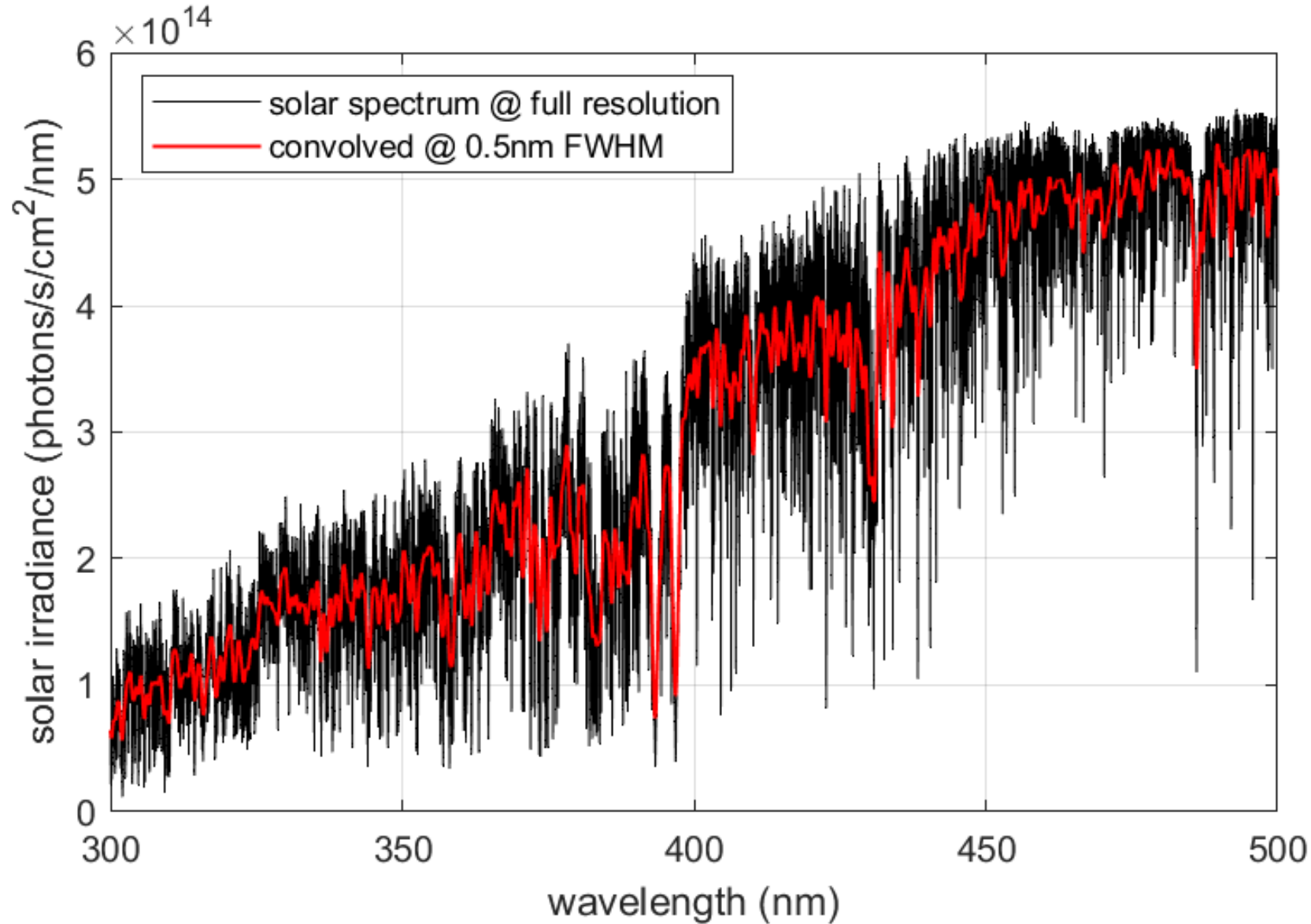
From the lab to the field

When a properly calibrated instrument is moved from the lab to the field (or launched into space), its characteristics can be altered due to various reasons, e.g.

- Changes in operating temperature affecting the optical response of the spectrometer
- Additional unwanted light (stray-light)
- Changes in the air pressure affecting refractive index (e.g. on balloon or aircraft)
- Doppler shift for satellite instruments moving fast relative to the sun
- Degradation due to aging of optical components
- ...

Fortunately a number of these effects can be mitigated using suitable retrieval approaches

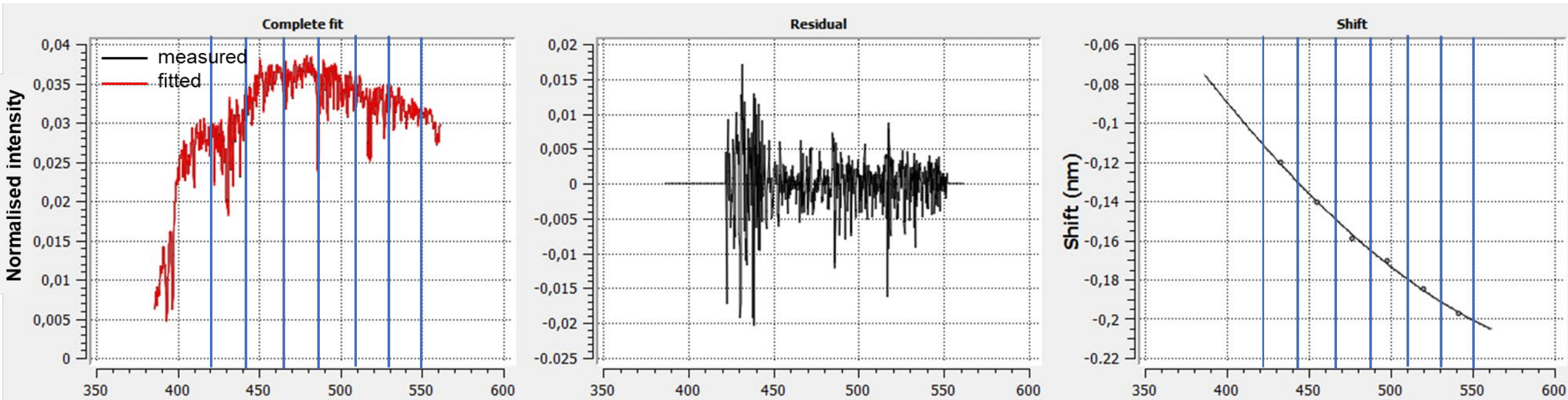
The sun as a light source



Joseph von Fraunhofer
(1787 – 1826)

Optimising the wavelength calibration in the field

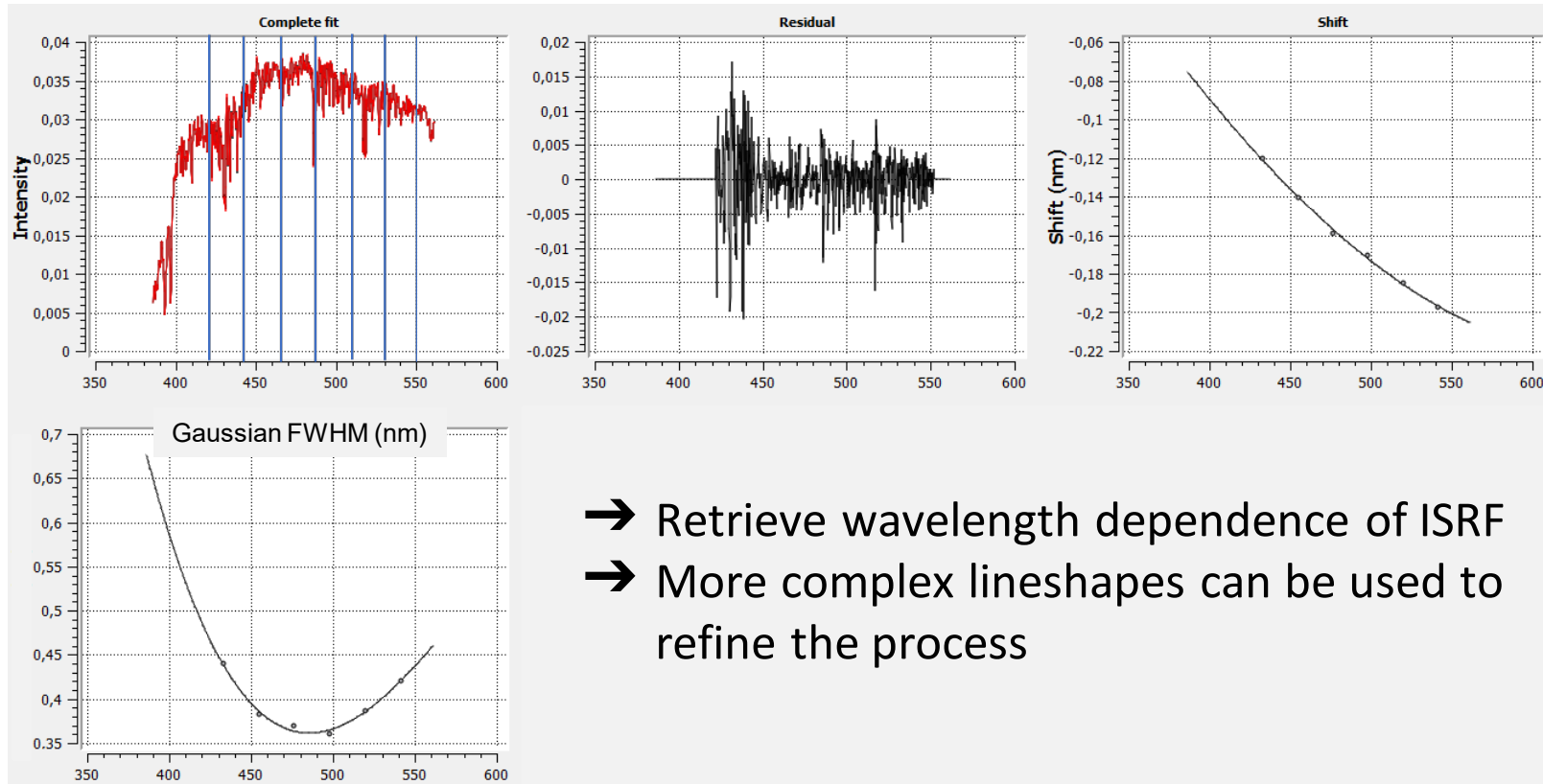
- Use atlas of solar lines (precisely known from literature) as wavelength reference
- Retrieve wavelength shift between measured spectrum and solar lines of known position in successive micro-windows, and use it to reconstruct an improved wavelength calibration



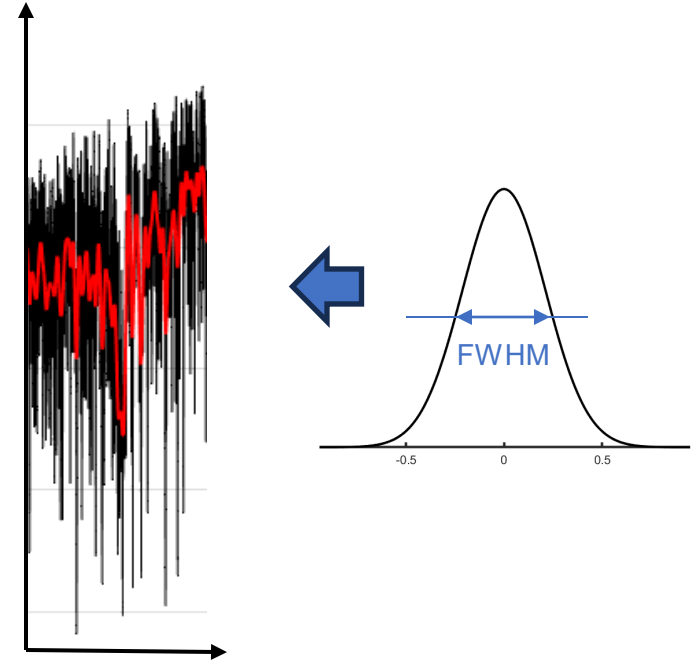
- This approach is very accurate (error < 0.01 nm) → usually more accurate than lab measurements

Optimising the ISRF (instrumental spectral response function)

- Same approach as for wavelength calibration, but...
- Start from high resolution solar atlas and apply dynamical convolution in each microwindow using a variable line shape (e.g. gaussian function)

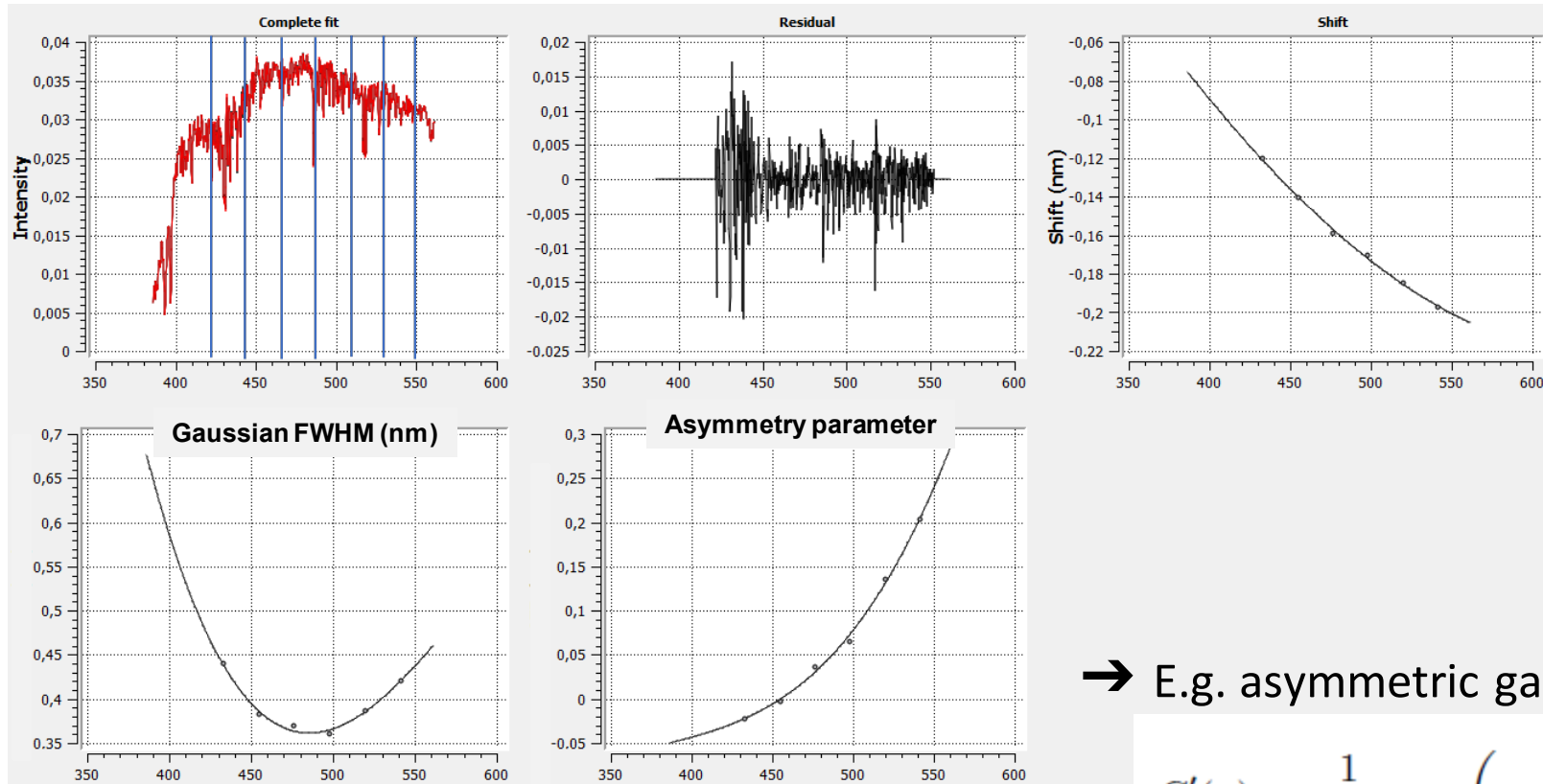


- Retrieve wavelength dependence of ISRF
- More complex lineshapes can be used to refine the process



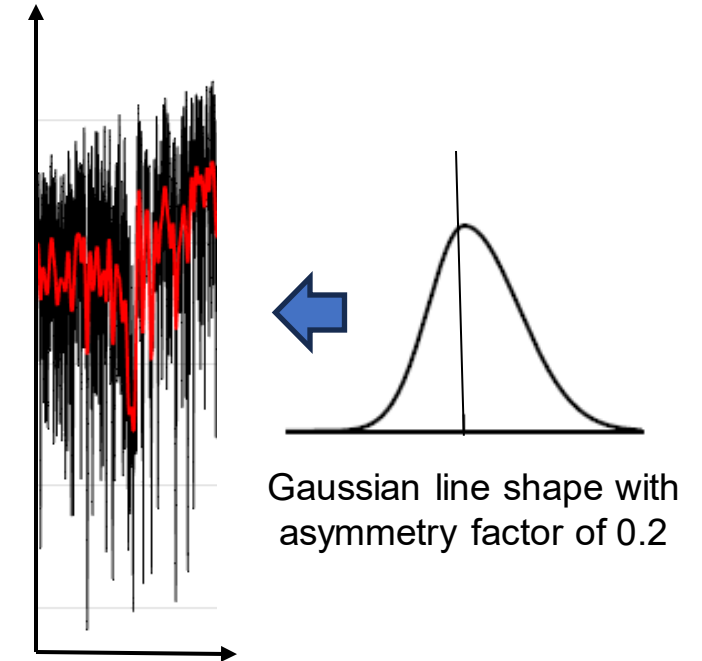
Optimising the ISRF (instrumental spectral response function)

- Same approach as for wavelength calibration, but...
- Start from high resolution solar atlas and apply dynamical convolution in each microwindow using a variable line shape (e.g. gaussian function)



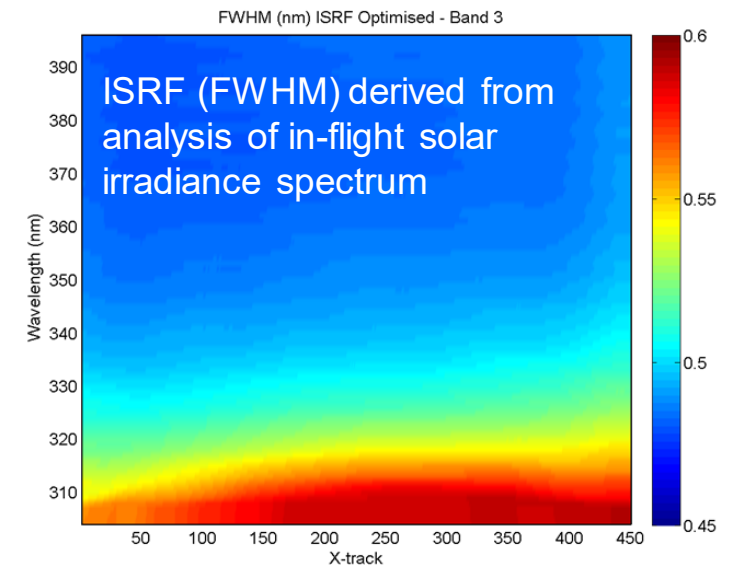
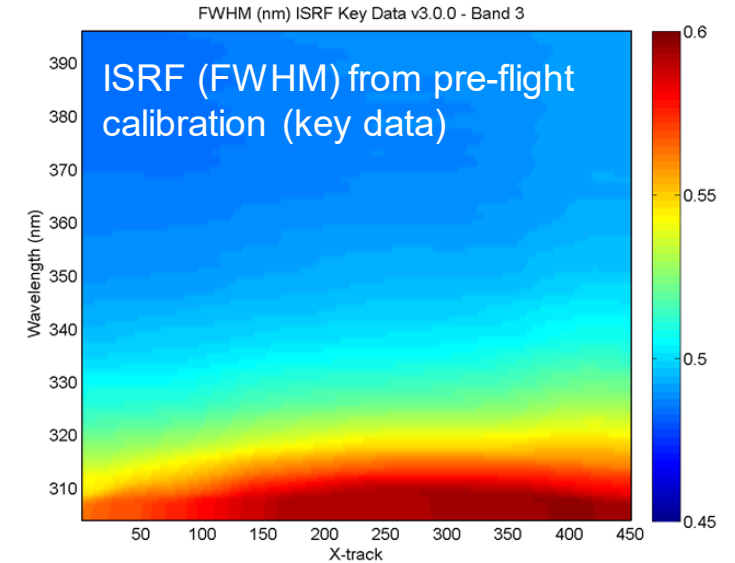
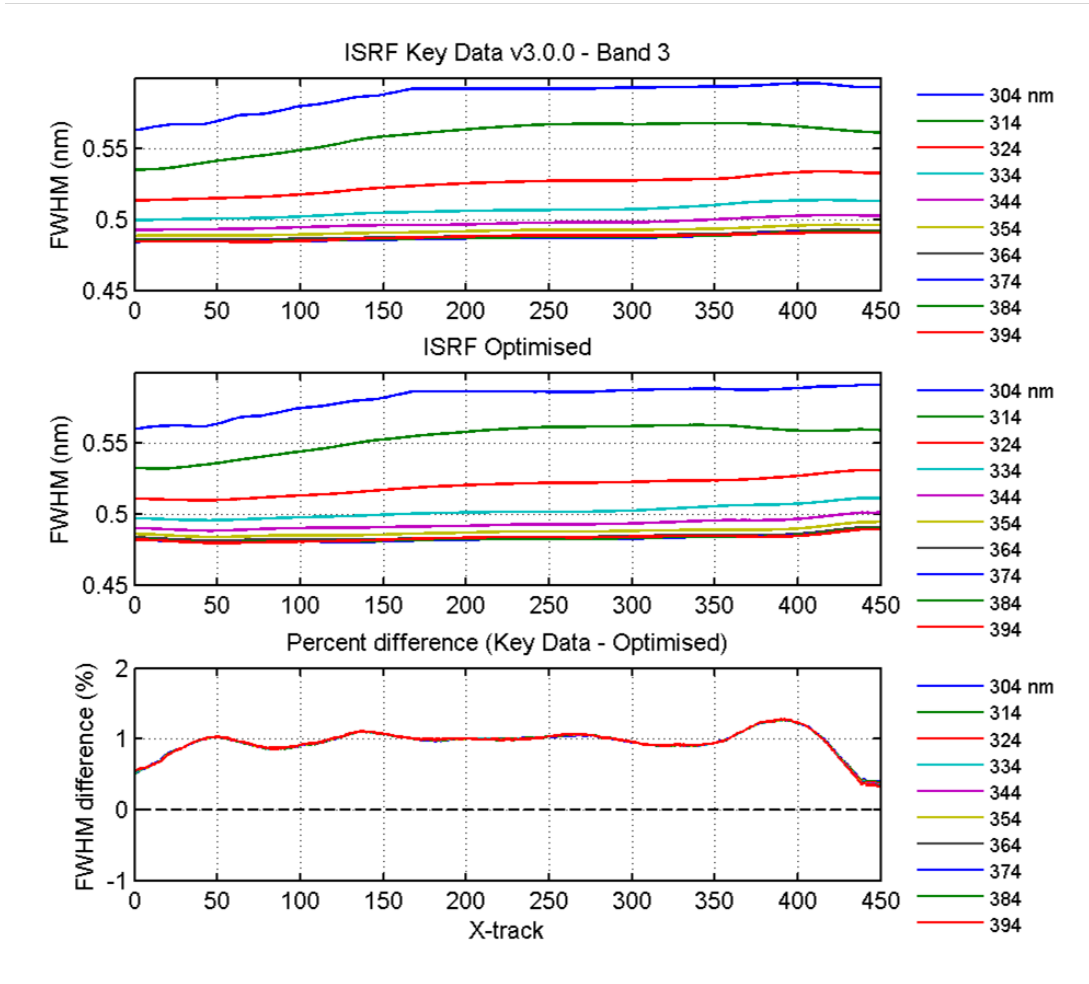
→ E.g. asymmetric gaussian line shape

$$G'(x) = \frac{1}{a\sqrt{\pi}} \exp\left(-\frac{x^2}{a^2(1 + \text{sign}(x)b)^2}\right)$$



Exemple: validation of Sentinel-5P/TROPOMI key data

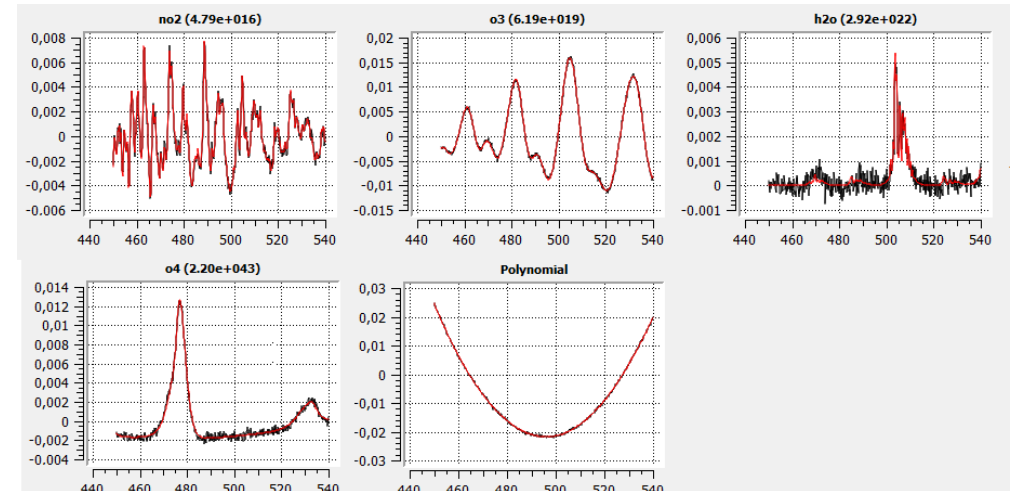
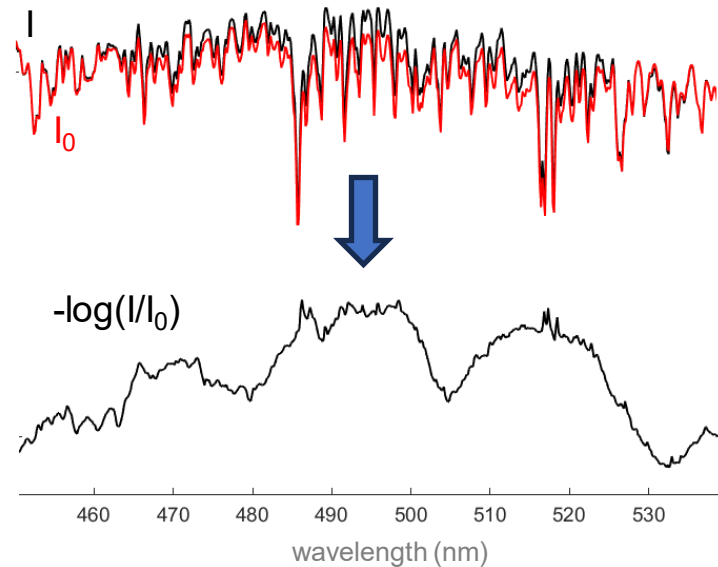
TROPOMI Band 3 (305-395 nm)



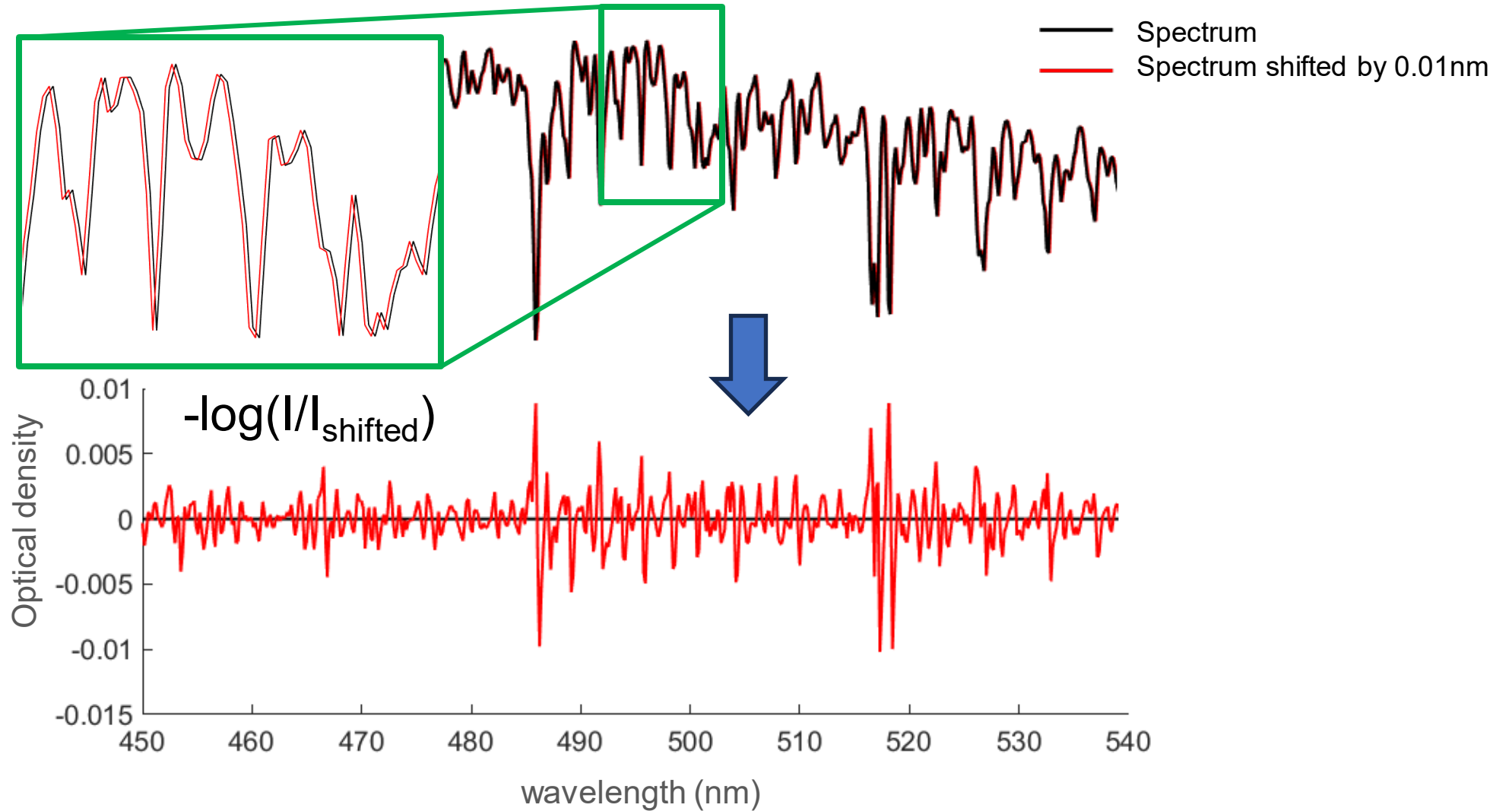
Atmospheric trace gas retrieval (DOAS)

Beer-Lambert law:
$$I(\lambda) = I_0(\lambda) \cdot e^{-\left(\sum_j \sigma'_j(\lambda) c_j - \left[\sum_i \sigma_{0j}(\lambda) c_j + \varepsilon_R + \varepsilon_M \right] \right)}$$
 Scattering terms (Rayleigh & Mie)

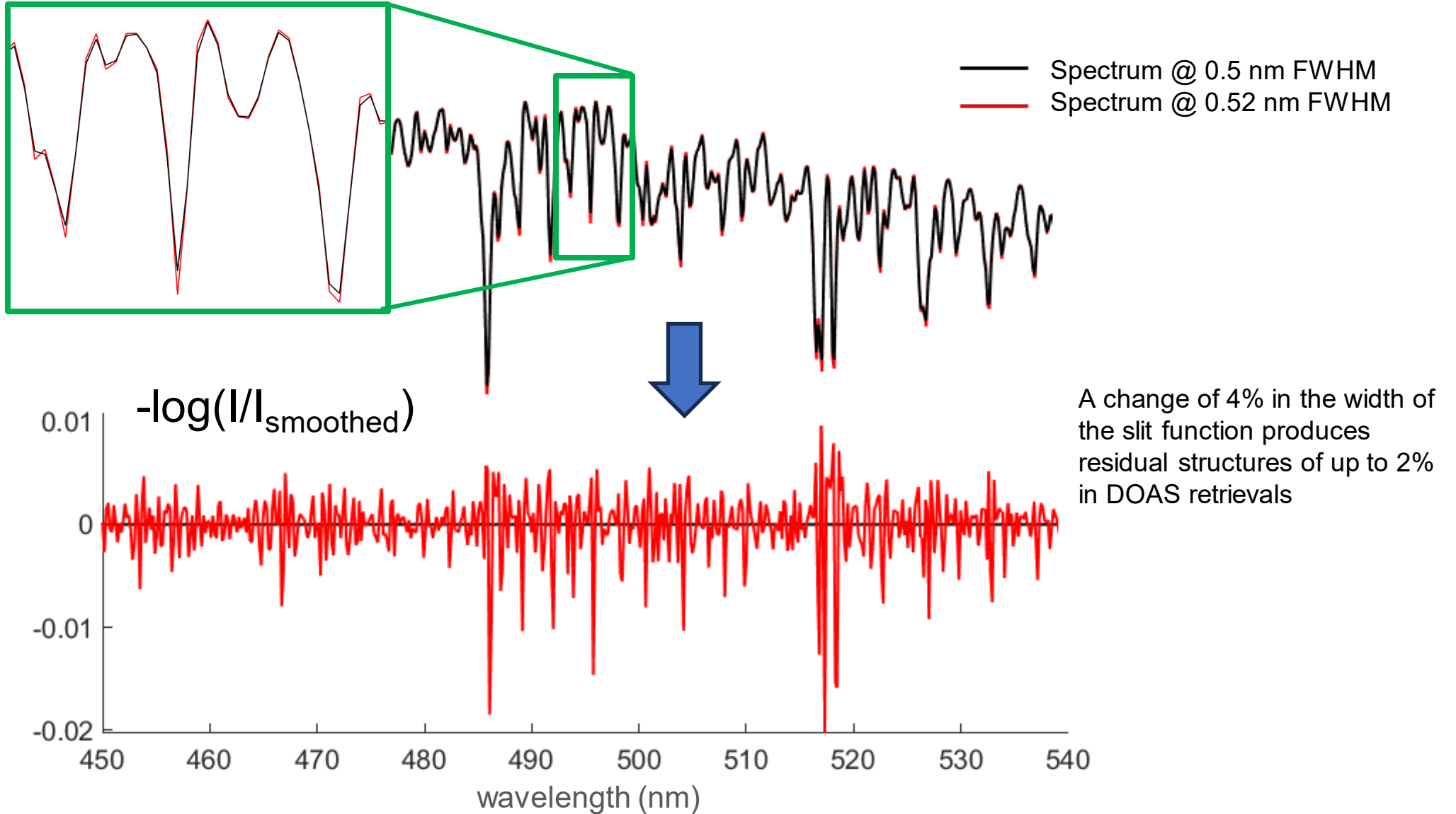
Optical density:
$$D_{\text{meas.}}(\lambda) = \ln \left(\frac{I_0(\lambda)}{I(\lambda)} \right) = \underbrace{\sum_j \sigma'_j(\lambda) c_j}_{\text{Structured Part} \rightarrow \text{trace gases}} + \underbrace{\left[\sum_j \sigma_{0j}(\lambda) c_j + \varepsilon_R + \varepsilon_M \right]}_{\text{Continuous Part} \rightarrow \text{polynomial function}}$$



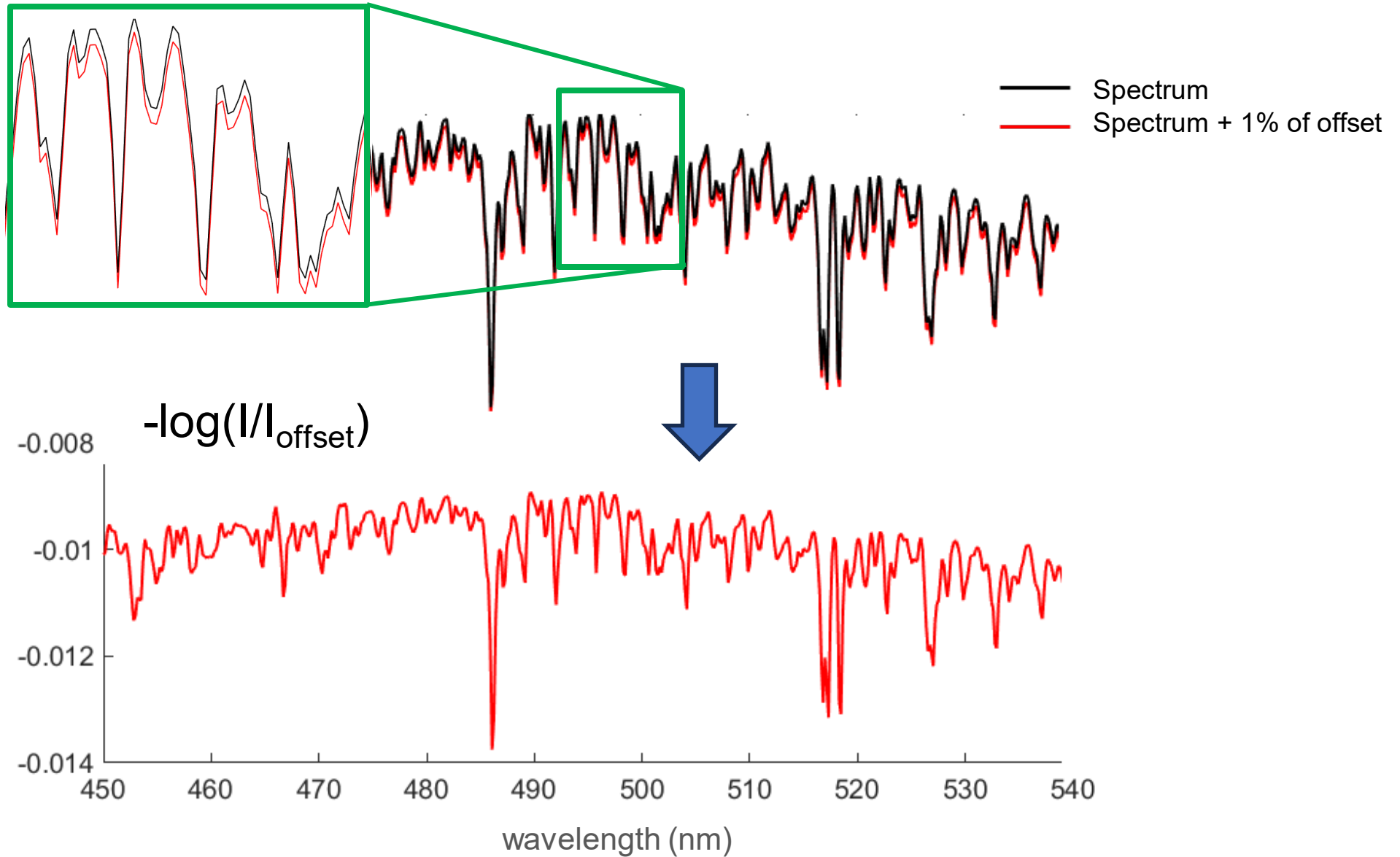
Spectral shift




Resolution change



Intensity offset



- 
- For all these effects, corrections can be implemented in DOAS retrievals softwares
 - Applicable to both ground-based and satellite instruments
 - Improves accuracy of retrievals and limits the impact of instrumental instabilities or degradation
 - If not properly corrected, these effects (or possible other ones) have a sizeable impact on the fitting residuals
 - Residuals from spectral fits provide an excellent diagnostic to detect instrumental issues, and this is routinely used for quality control

E.g. Monitoring of instrumental degradation og GOME-2

Analysis of changes in the noise of the retrieved trace gas columns, or changes in monitored slit function parameters

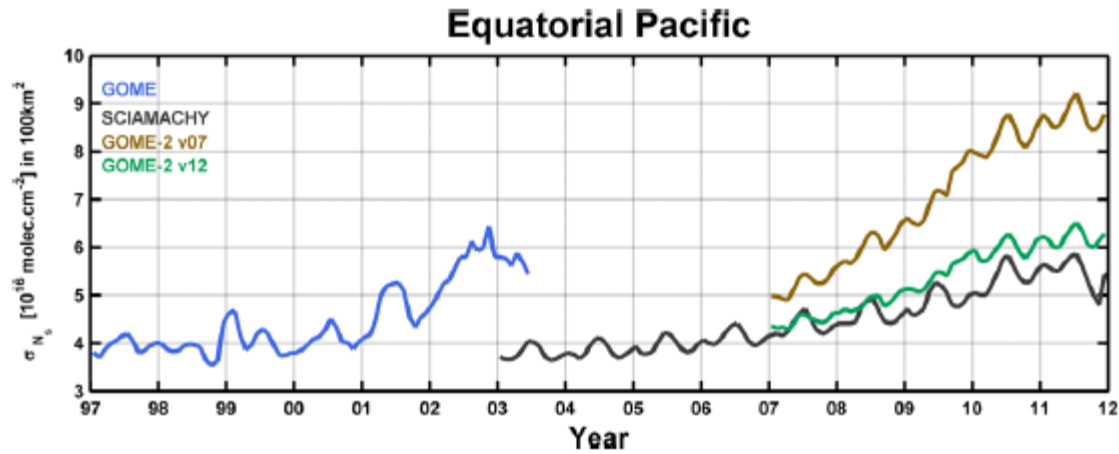


Fig. 3. H₂CO slant column standard deviation scaled to a pixel size of 10 × 10 km², retrieved from GOME, SCIAMACHY and GOME-2 over the equatorial Pacific. Two versions of GOME-2 results are shown: the initial retrieval settings (v07) and the improved settings (v12, see text for details).

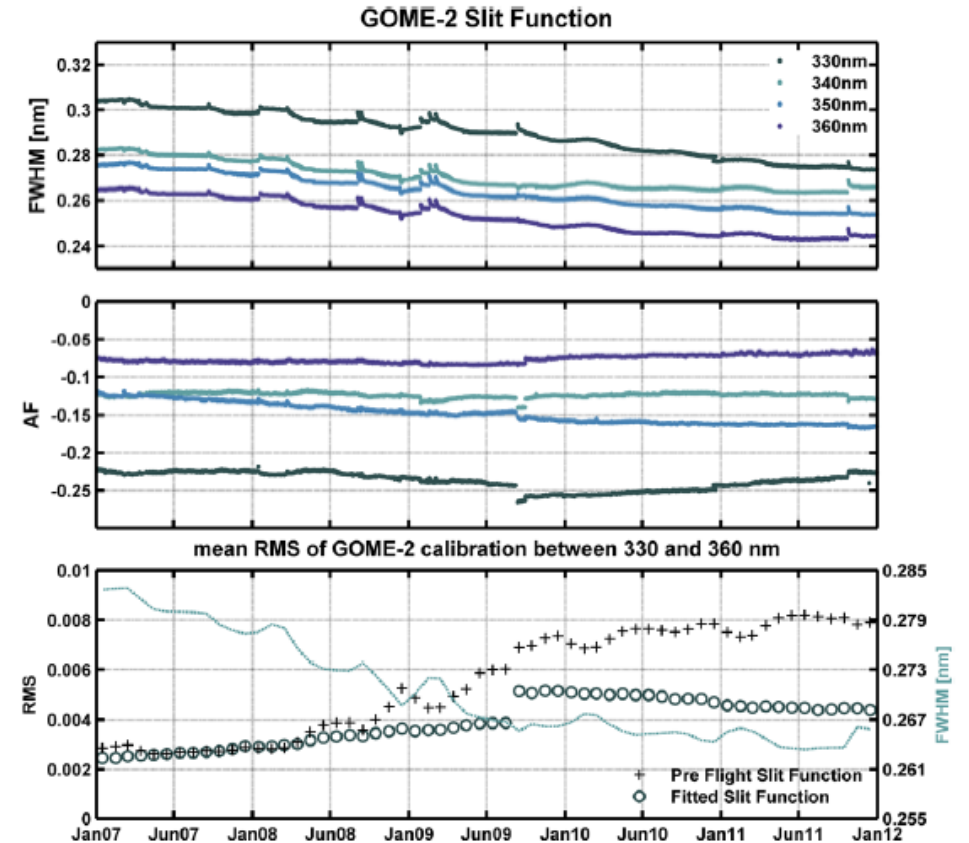


Fig. 6. (a) GOME-2 slit function width (FWHM) and asymmetry factor (AF) fitted during the calibration procedure of the DOAS analysis. (b) Mean residuals of the GOME-2 solar spectrum calibration between 330 and 360 nm, using the pre-flight slit function or fitting a Gaussian asymmetric slit function. The FWHM of the fitted Gaussian asymmetric slit function is shown as second y-axis.

Soft-calibration of satellite nadir reflectances

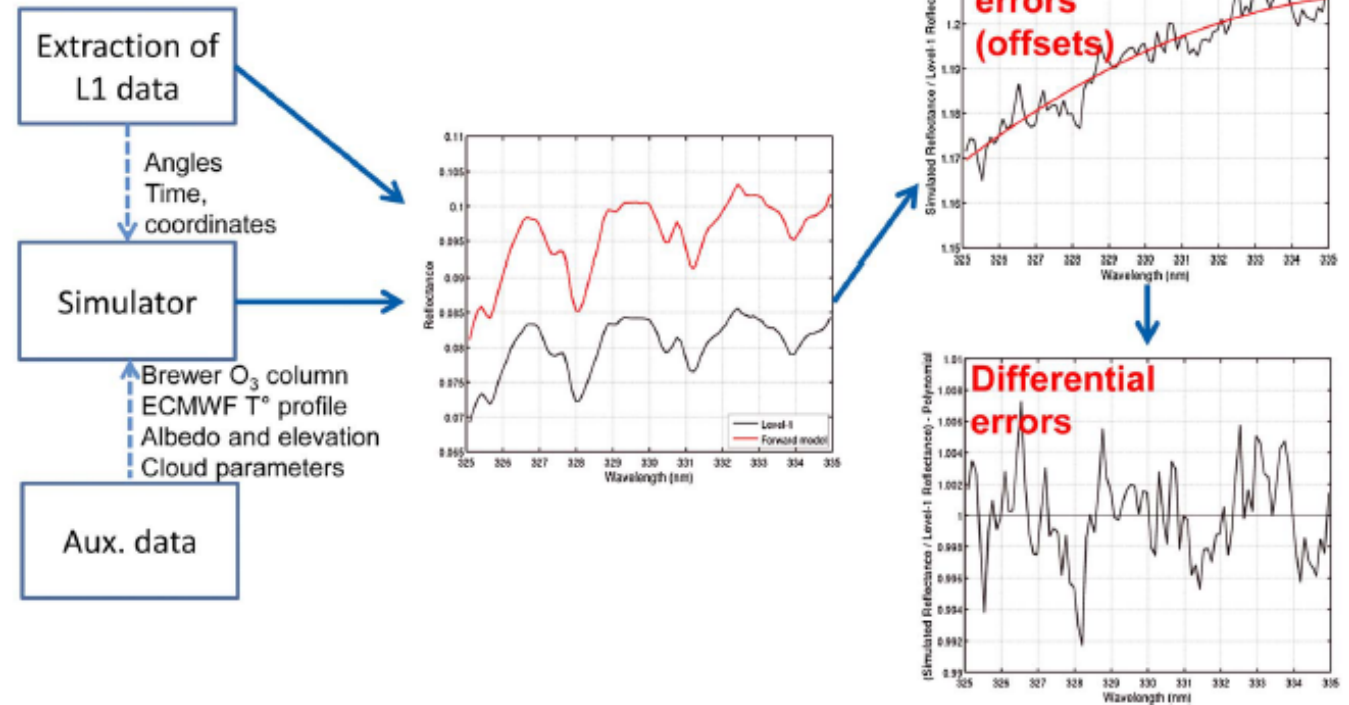
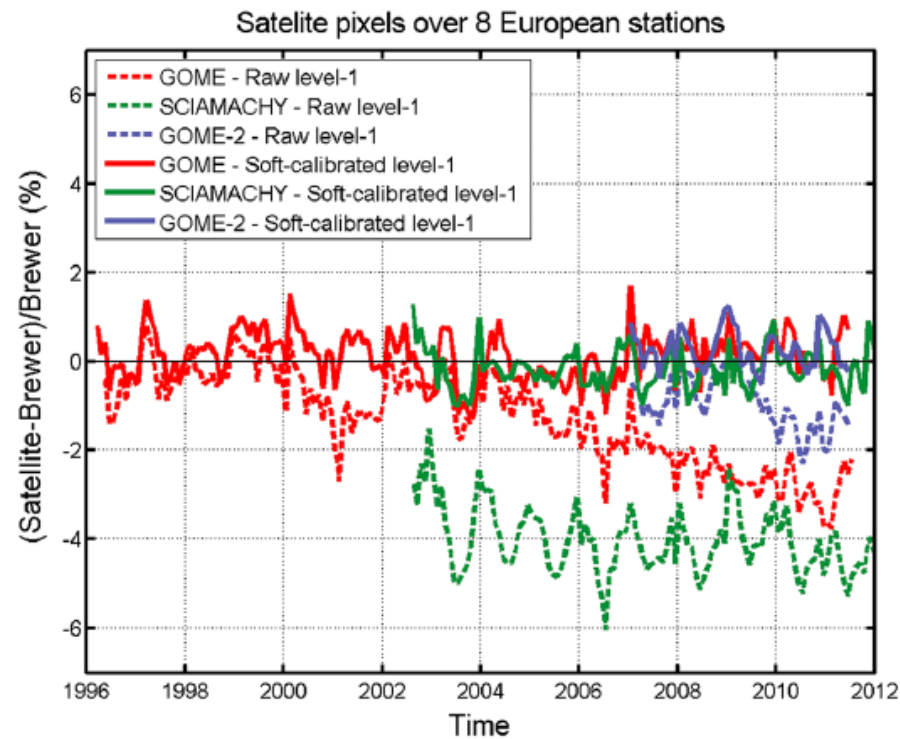
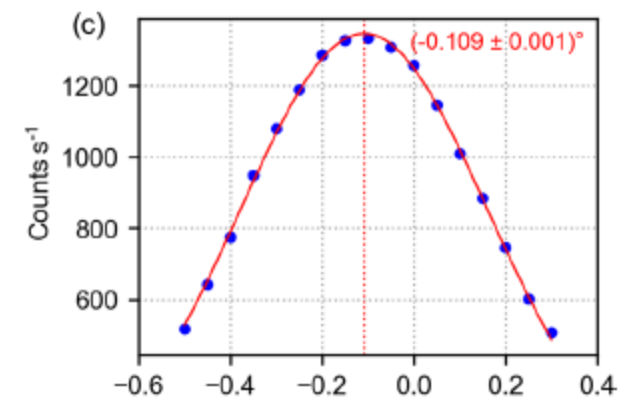
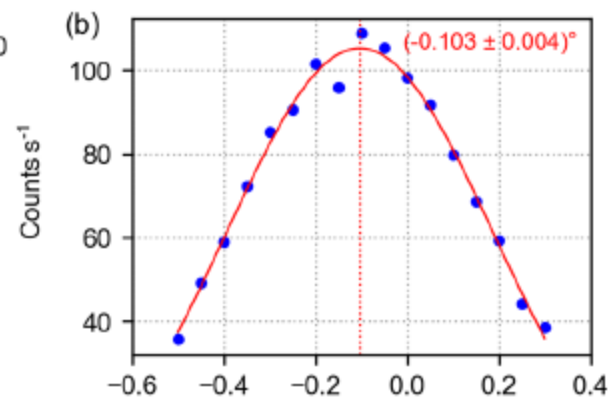
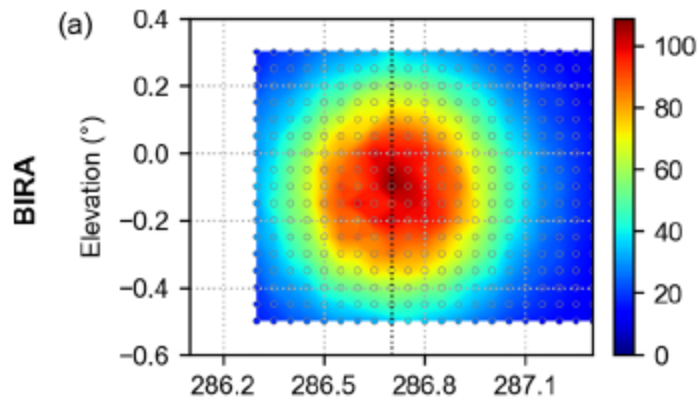
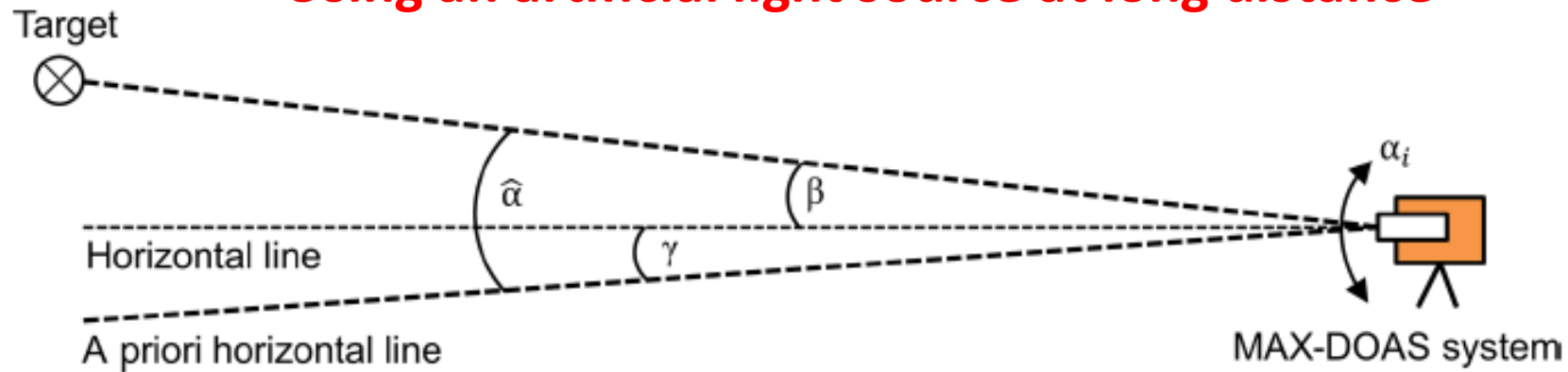


Figure 8. Sketch illustrating the possible detection of radiometric calibration (absolute) errors and artificial spectral features (differential errors). For each satellite scene in colocation with a Brewer measurement, a simulated spectrum is compared to the level-1 reflectance. A low-order polynomial fitted through the ratio of the spectra discriminates broadband effects from the high-frequency features.

In-field calibration of MAX-DOAS scanners

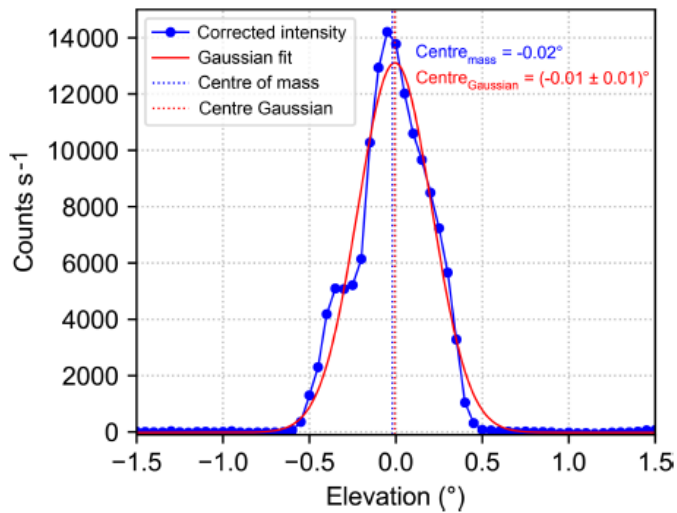
Using an artificial light source at long distance



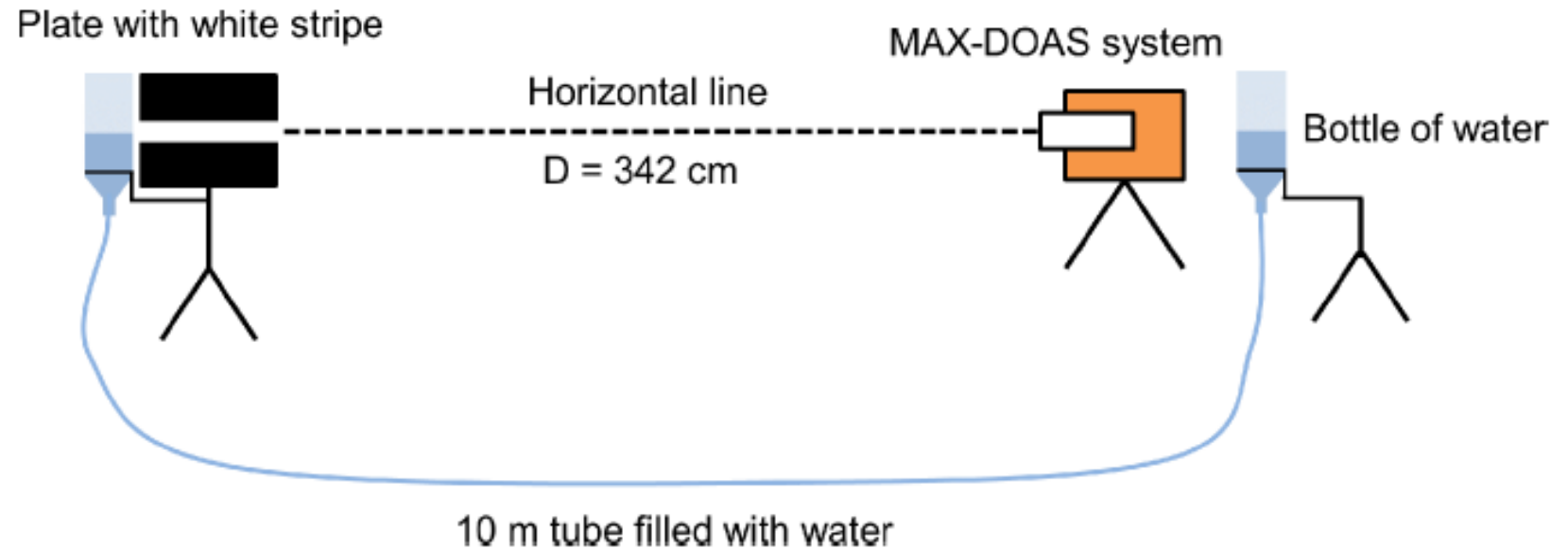
Accuracy $\pm 0.05^{\circ}$

In-field calibration of MAX-DOAS scanners

Using a black board with a white stripe

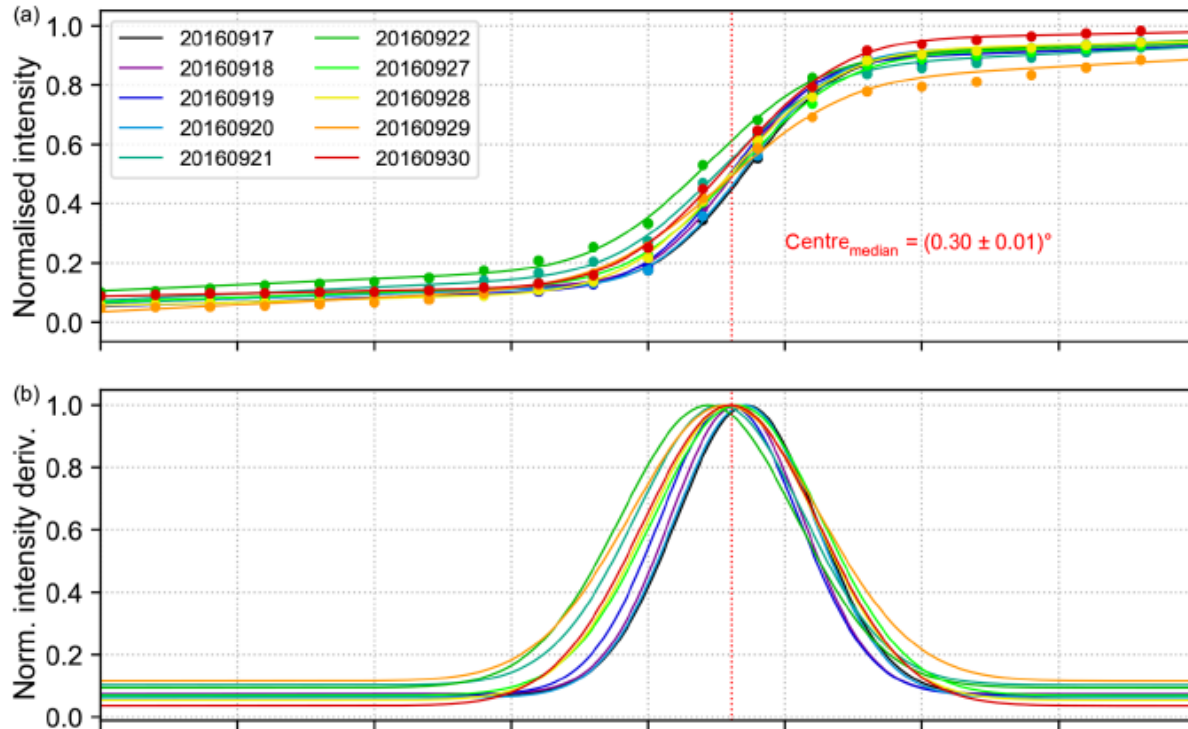


Accuracy $\pm 0.1^\circ$



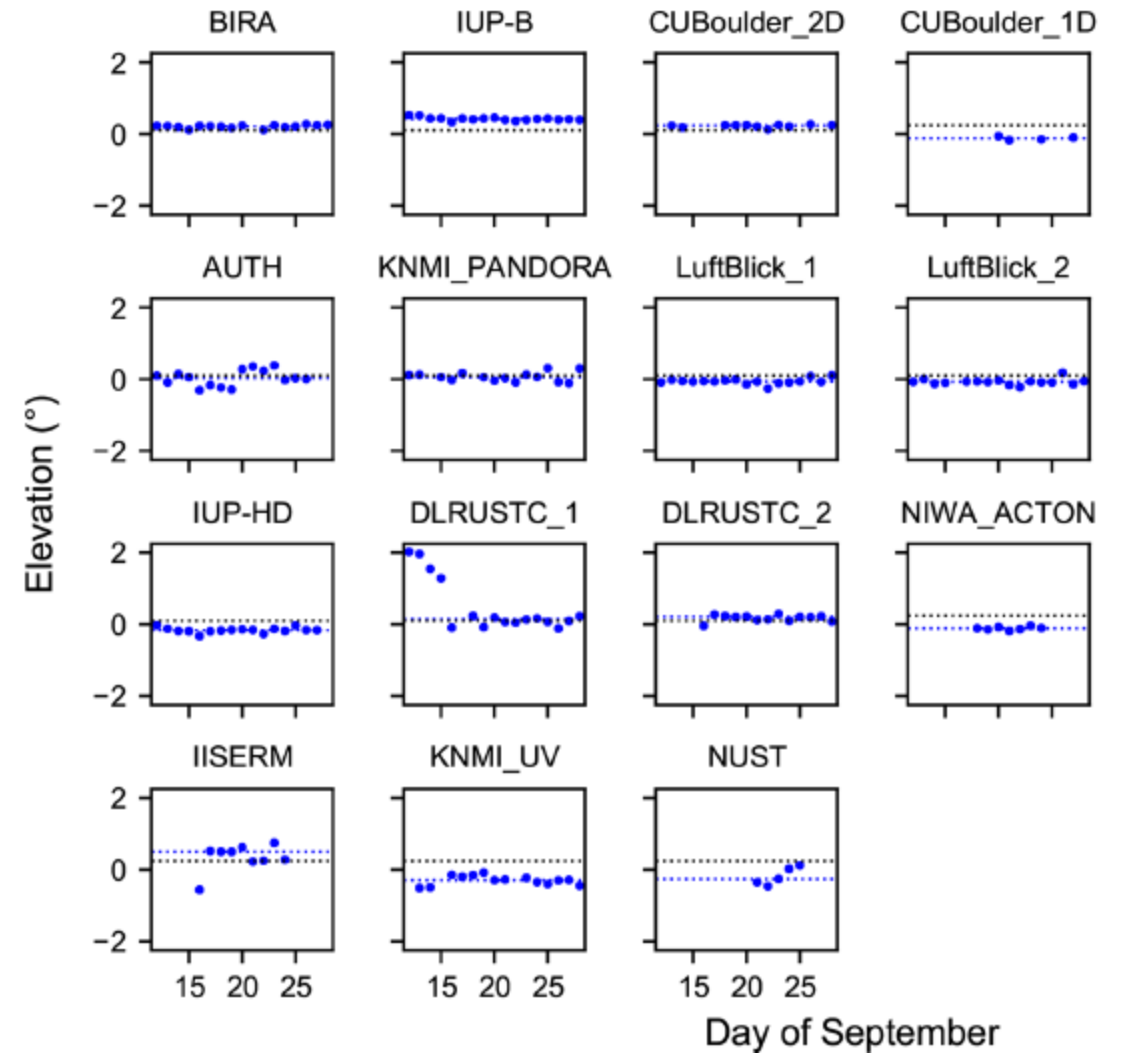
In-field calibration of MAX-DOAS scanners

Using horizon scans



Accuracy limited ($\pm 0.25^\circ$) but useful for regular monitoring

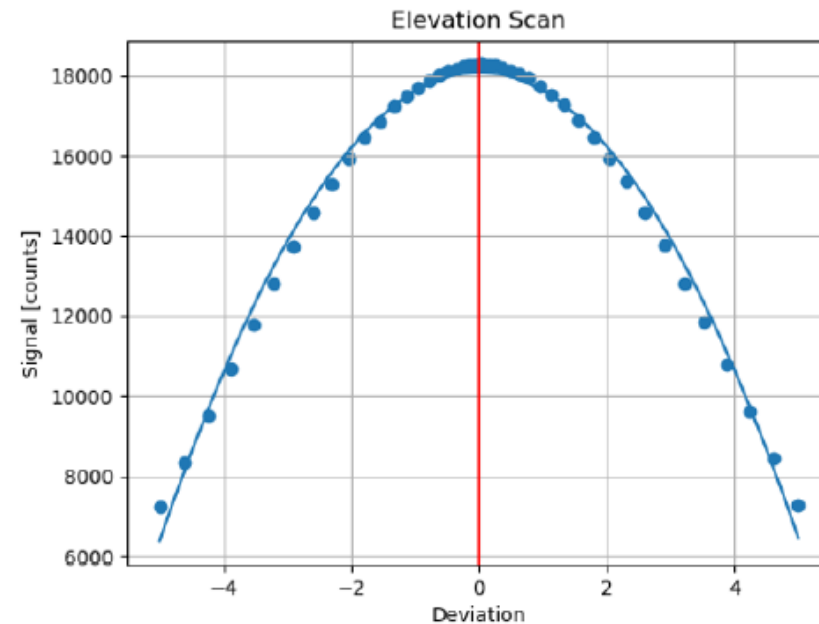
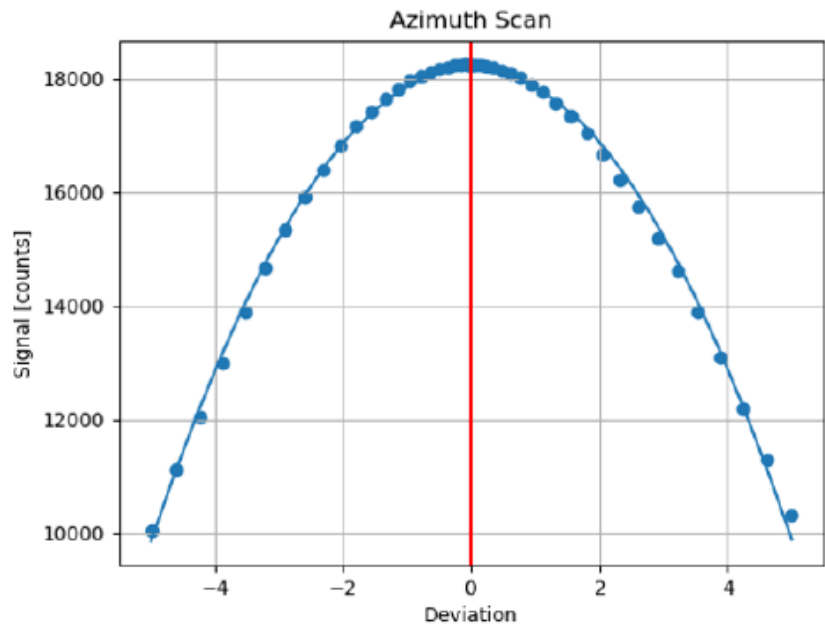
CINDI-2 campaign, Cabauw, Sep 2016



In-field calibration of MAX-DOAS scanners

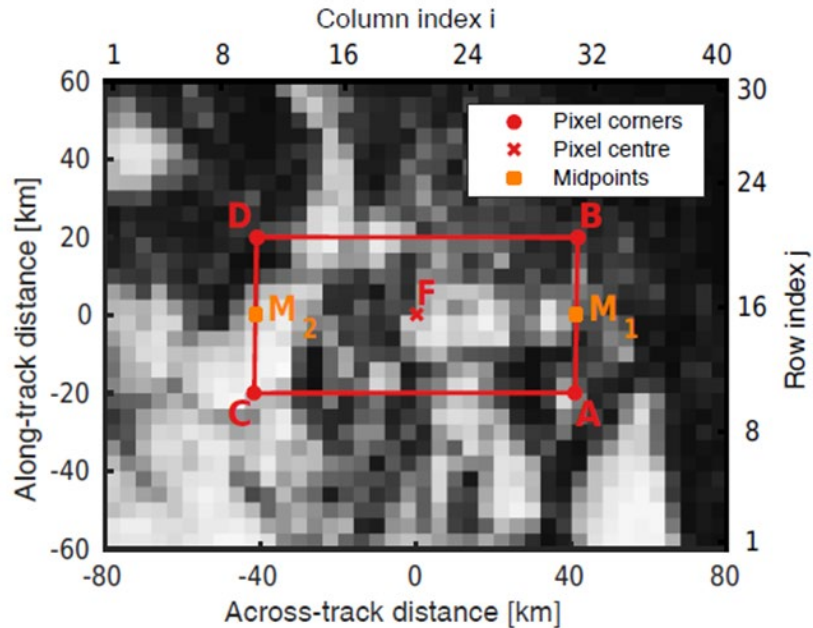
Using sun scans

- Allows for calibration of both elevation and azimuth axes
- Best accuracy ($\pm 0.05^\circ$) and can be repeated regularly for monitoring
- Only applicable to systems equipped with 2D scanners and direct-sun optics



In-operation satellite field-of-view (FOV) retrieval

- Idea:** → simultaneously record the same scenes using sensors of low and high-resolution
 → the FOV of the low-resolution sensor can be derived using multiple joint measurements with both systems



$$\begin{pmatrix} l_1 \\ \vdots \\ l_m \end{pmatrix} = \begin{pmatrix} 1 & h_{11} & \cdots & h_{1n} \\ \vdots & \vdots & & \vdots \\ 1 & h_{m1} & \cdots & h_{mn} \end{pmatrix} \begin{pmatrix} c_0 \\ c_1 \\ \vdots \\ c_n \end{pmatrix}$$

Application to GOME-2 FOV retrieval

$$l_i = c_0 + \sum_{j=1}^n h_{ij} c_j$$

